MASARYKOVA UNIVERZITA
Přírodovědecká fakulta
Ústav teoretické fyziky a astrofyziky

Bakalářská práce

Brno 2014 Tomáš Procházka

MASARYKOVA UNIVERZITA
Přírodovědecká fakulta
Ústav teoretické fyziky a astrofyziky

CCD fotometrie vybraných otevřených hvězdokup

Bakalářská práce

Tomáš Procházka

Vedoucí práce: doc. RNDr. Miloslav Zejda, Ph.D. **Brno 2014**

Bibliografický záznam

Autor:	Tomáš Procházka Přírodovědecká fakulta, Masarykova univerzita Ústav teoretické fyziky a astrofyziky
Název práce:	CCD fotometrie vybraných otevřených hvězdokup
Studijní program:	Fyzika
Studijní obor:	Fyzika
Vedoucí práce:	doc. RNDr. Miloslav Zejda, Ph.D.
Akademický rok:	2013/2014
Počet stran:	ix+43
Klíčová slova:	hvězdná fotometrie, CCD fotometrie, hvězdokupy, HR diagram, otevřené hvězdokupy

Bibliographic Entry

Author:	Tomáš Procházka Faculty of Science, Masaryk University Department of theoretical physics and astrophysics
Title of Thesis:	CCD photometry of selected open clusters
Degree Programme:	Physics
Field of Study:	Physics
Supervisor:	doc. RNDr. Miloslav Zejda, Ph.D.
Academic Year:	2013/2014
Number of Pages:	ix+43
Keywords:	stellar photometry, CCD photometry, star clusters, HR diagram, open clusters

Abstrakt

V této bakalářské práci budou na základě výsledků CCD fotometrie studovány vybrané otevřené hvězdokupy Chupina 1, Chupina 2 a M67.

V teoretické části budou shrnuty dosavadní poznatky o hvězdokupách, jejich typech i vlastnostech a klasifikaci otevřených hvězdokup. Také bude vysvětlena metoda hvězdné fotometrie, HR diagram a CCD fotometrie, které využijeme při samotném měření.

Praktická část je zaměřená na data získaná z měření otevřených hvězdokup. Z naměřených dat bylo určeno stáří a vzdálenost jednotlivých hvězdokup. V závěru je provedeno srovnání získaných výsledků a aktuálních hodnot publikovaných v odborných článcích.

Abstract

In this bachelor thesis open clusters Chupina 1, Chupina 2 and M67 will be studied using the results of CCD photometry.

In theoretical part there will be summarized our knowledge of clusters, their types and characteristics and classification of open clusters as well. There will be also explained the method of stellar photometry, HR diagram and CCD photometry, which will be used during the measurement.

The practical part is focused on data gained from the measurement of open clusters. From measured data the ages and distances of individual open clusters were determined. In conclusion there is a comparation of the gained results with actual values published in scientific papers.

Masarykova univerzita

Přírodovědecká fakulta

ZADÁNÍ BAKALÁŘSKÉ PRÁCE

Student: **Tomáš Procházka**

Studijní program: **Fyzika**
Studijní obor: **Fyzika**

Ředitel Ústavu fyzikální elektroniky PřF MU Vám ve smyslu Studijního a zkušebního řádu MU určuje diplomovou práci s tématem:

CCD fotometrie vybraných otevřených hvězdokup

CCD photometry of selected open clusters

Oficiální zadání: Student získá vlastní CCD pozorování alespoň jedné otevřené hvězdokupy, případně využije dosud nezpracovaná data jiných pozorovatelů, provede základní zpracování CCD dat a jejich analýzu. Pomocí nástrojů databáze WEBDA pak určí parametry studovaných otevřených hvězdokup.Práce bude vyhotovena v anglickém jazyce.

Jazyk závěrečné práce: angličtina
Vedoucí bakalářské práce: RNDr. Miloslav Zejda, Ph.D.
Podpis vedoucího práce: Zejda
Konzultant:
Datum zadání bakalářské práce: listopad 2013

V Brně dne 18. 11. 2013

Prof. RNDr. Mirko Černák, CSc.
ředitel Ústavu fyzikální elektroniky

Zadání bakalářské práce převzal dne: 21. 11. 2013

Podpis studenta: Procházka

Acknowledgements

I would like to express my thanks to doc. RNDr. Miloslav Zejda, Ph.D. for his guidance through my bachelor thesis, valuable comments and patience. My thanks belong to Ondrej Kamenský, who instructed me during my difficulties. I would like to thank also RNDr. Jan Janík, Ph.D. and Mgr. Filip Hroch, Ph.D. for their valuable advices about data processing, Mgr. Jiří Liška for his guidance during my measurement and his helpful advices and at last but not at least my closest ones for supporting me all that time.

Statement

I declare that I developed my bachelor thesis independently with the use of information sources, which are in the work cited. I agree with publishing my work and with lending it as well.

Brno 20. května 2014 ....

Tomáš Procházka

Contents

Symbols and conventions

For better orientation in text there is a summary of symbols and conventions, which are used in the work.

$1\,ly$	Light-year. The distance which light travels per one year. $1\,\mathrm{ly} \approx 9.46 \cdot 10^{15}\,\mathrm{m}$.
$1\,pc$	Parsec. The distance from which we see an object with a lenght of 1 AU under the angle of $1''$. $1\,\mathrm{pc} = 3.26\,\mathrm{ly}$.
$1\,Gyr$	Giga-year. $1\,\mathrm{Gyr} \doteq 10^9$ years.

By using term *Galaxy* we mean our galaxy, Milky Way. Term *galaxy* means any galaxy.

Chapter 1

Clusters

One of the biggest structures in the universe are galaxies. There are several types of galaxies, for example our galaxy - the Milky Way - is a spiral galaxy. Its components are nucleus, the disc containing spiral arms and the outer halo which envelopes the whole galaxy. Nucleus makes the core of the Galaxy with a great mass, which makes (by its gravitational field) other objects located mostly in the disc and spiral arms rotate around the center of the Galaxy. Those objects are mainly stars, gas and dust.

Stars in galaxies are not isolated objects, some of them attract other stars by their gravitational forces creating star systems with relatively small extent. Such groups of stars we call star clusters. Due to the gravitational forces of their members, star clusters take relatively small space in comparation with the size of the Galaxy. This fact makes stars from star clusters be in appproximately the same distance from Earth.

1.1 Types of star clusters

There are two main types of clusters - globular clusters and open clusters. The type of a cluster is based on its shape. Globular clusters are formed into a large sphere, on the other hand, open clusters do not make any specific shape. We can hardly find the border of these open clusters, that is why we call them open clusters.

Besides those two types, we can also talk about extragalactic clusters and asterisms. Extragalactic clusters are clusters located in different galaxies, on the contrary, asterisms are not clusters at all - these are stars we see on the night sky very close to each other, but in fact, the distance from Earth can be different for each particular star.

There are several more types of star clusters, but they are quite rare, therefore, we will not mention them any further.

1.1.1 Globular clusters

Globular clusters are structures located in the galaxy halo. They may contain over a milion stars. With so many members, the object is formed into a huge sphere by gravitational forces of stars included. Globular clusters were created from the original nebulous gas soon after the formation of our Galaxy. They trace its original extent from the beginning of the Galaxy defining the outer area of the Milky Way.

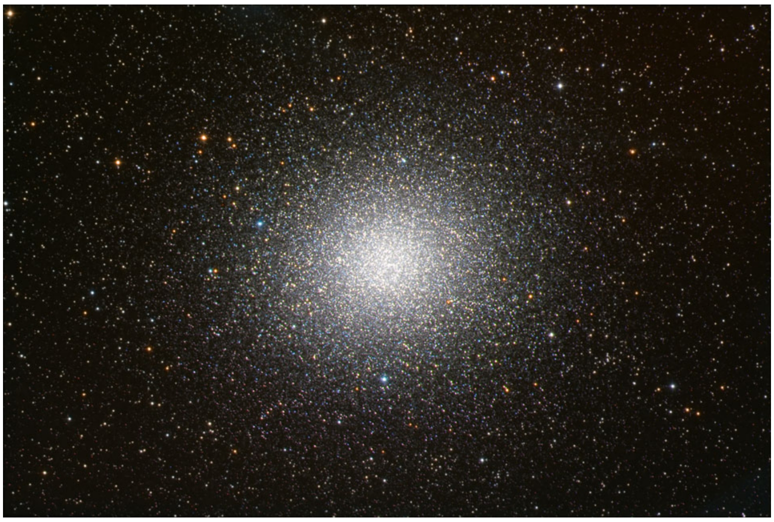

Fig. 1.1: Globular cluster Omega Centauri [e1]

The age of the oldest stars in globular clusters can go up to 15 Gyr. Therefore, it is thought that the halo was the original extent of the galaxy and was formed as first by collapsing the gas in on itself, which provided home for first stars and later globular clusters. However, other theories say that some of our globular clusters were in the past members of dwarf galaxies and our galaxy "stole"them through milions and billions of years [1]. The origin of the globular clusters, however, is out of scape of this thesis.

1.2 Open clusters

Open clusters are relatively young structures in the Galaxy. On the contrary to globular clusters, open clusters contain much less stars. They are stationed in the galactic disc randomly. All stars of every particular open cluster were created from one and the same molecular cloud. The gas and dust contracted under gravity rapidly, coalescing into fragments and eventually each fragment forming a new star. The formation of a star is relatively short process in comparation with the actual age of stars (except very young stellar associations), that is why all stars in one open cluster can be assumed to be the same age. Being created from the same molecular cloud, stars in one open cluster have very similiar chemical composition.

Fig. 1.2: Pleiades open cluster [e2]

1.2.1 Open clusters remnants

Though open cluster do not have any specific shape, they do have an organized structure. The most massive bright stars make the nucleus, on the other hand, fainter stars make the corona. Through time, thanks to the gravitational forces from within our Galaxy, the stars in the corona are getting less affected by each other and they begin to leave the cluster. We call this effect evaporation of clusters. Later, only the most massive stars are left in the cluster, because their gravitational forces are still strong enough to keep them together. This final stage of open clusters we call open clusters remnants. Later, even cluster remnants are completely evaporized.

1.3 Characteristics of open clusters

1.3.1 The age of open clusters

The maximum age of one open cluster depends on the masses of stars contained. Usually, open clusters have ages less than 10 Gyr [2]. However, thanks to the affection of gravitational forces from within our Galaxy and possible collisions of stars, open clusters relatively quickly evaporize and only a few of them reaches the age of one billion years.

Because stars in open clusters belong to the youngest object in the Galaxy, they contain much more heavier elements then their globular metal-poor cousins. Mostly main sequence stars are found in open clusters, which can tell us a lot about the life of main seqence stars.

There are from dozens to several hundrets of stars in open clusters and so the total luminosity of open clusters equals hundrets of Ł$_\odot$. The record may be, however, about 50 000 $L_\odot$ [3].

1.3.2 Size and number of open clusters

As mentioned, each star of an open cluster is approximately in the same distance from Earth, which makes open clusters relatively small structures in comparison with the size of the Galaxy. Their size goes from 2 to 75 ly and component stars are tightly packed with space of about 1 ly between them [4]. There are over 2000 known open clusters in our Galaxy [5]. Small size plus large interstellar absorption, however, may be causing that lots of open clusters within our Galaxy remain undiscovered.

1.3.3 Uses of study

Studying of open clusters can be useful for several reasons [6]:

- Investigating the shape and dynamics of the Galaxy.
- Setting the distance scale in our Galaxy by which we can calibrate other distance indicators.
- Studying star formation history of the Galaxy.
- Predicting of evolution in the Galaxy.
- The research of stars

and more.

1.4 Classification of open clusters

Open clusters can be classified according to their parameters. We use the classification system of Trumpler (1930). The division is according to three criteria:

According to **central concentration**

- I - detached and strong central concentration
- II - detached and little central concentration
- III - detached and no central concentration
- IV - not detached from outer stars, merges into the star field

According to **brightness**

- 1 - small brightness range
- 2 - medium range
- 3 - vast brightness range

According to **richness** (poor, moderate, rich)

- p - poor, less than 50 stars
- m - moderate, 50 to 100 stars
- r - rich, more than 100 stars

A final letter n, is used when a nebula is included.

1.5 Spectral classification of stars

By comparing spectra of various stars we can see that some spectra are very similiar and we can divide stars into several spectral classes. In the past, stars were divided into spectral classes according to their visual characteristics. For example H. C. Vogel in 1874 published the spectral classification based on the idea that spectra are related with ages of the stars [7]. First, who started to divide the stars into classes was P. A. Secchi and even nowadays we can still use Secchi's classification, although only for brief and quick characteristics. However, the classification published by Vogel is not being used anymore.

After the improvement in the area of photography, the method of spectral photography started to push away all visual methods. E. C. Pickering, with the assistance of miss Maury and others, was leading the work on the Harvard's observatory about spectral classification of stars. The result was the list of stellar spectra called *Henry Draper Catalgoue* including more then 225 000 stars.

Spectral classes of HD catalogue classification are selected with the capitals

$$O\,B\,A\,F\,G\,K\,M\,L\,T\,Y,$$

but most of the spectras are divided into classes $O\,B\,A\,F\,G\,K\,M$. Letters L, T and Y are related to spectra of cold objects. Spectra of individual stars are not exactly identic. In every spectral class we can see differences, which mean that stellar spectra can slowly go from one class to another in the row. For dividing different spectra of one class we put the number from 0 to 9 behind a letter related to the spectral class; for example B0 is almost O9 and B9 is going to A0. For example, our Sun is described by spectral class G2. Sometimes we meet anomalies, which cannot be desribed by any criteria used for selecting the star into the spectral class. For these cases we add to the name of the class another letter [8]:

- n - nebulous. Spectral lines are difused.
- s - spectral lines are sharp.
- g - the spectrum indicates the marks of a giant.
- d - indicates a dwarf star.
- e - the presence of emission spectral lines.
- w - indicates a white dwarf

and more.

Stars of class M and higher are known as cold ones. Morgan-Keenan's classification adds to a spectral class also the class of luminosity (I-VII):

- Ia - bright supergiants
- Ib - supergiants.
- II - bright giants.
- III - giants.
- IV - subgiants.
- V - main sequence stars.
- VI - subdwarves.
- VII - white dwarves.

Open clusters contain mostly (but not only) main sequence stars.

Chapter 2

Stellar photometry

Basic tool of stellar astrophysics - the stellar photometry - helps to determine the age, chemical composition and distance of open clusters.

2.1 Electromagnetic radiation

Electromagnetic radiation is one of the most important phenomenons of every object of the universe. We can see the light coming from the stars, for example. Light, however, is not the only electromagnetic radiation. Our measuring devices can, in addition, recognize X-rays, gamma, ifrared, ultra-violet, microwave or radio radiation. The type of electromagnetic radiation depends on a wavelenght λ, in which the source shines. The wavelenght is closely related with the frequency ν:

$$\lambda = \frac{v}{\nu}, \tag{2.1}$$

where v is the speed of the radiation. In stellar photometry, we can assume that electromagnetic radiation spreads through vacuum, which means that we can put $v = c$, where c is the speed of light in vacuum ($c = 2.99792458 \cdot 10^8\,\mathrm{m\,s^{-1}}$).

Quantum theory says that electromagnetic radiation is made by quanta, which we call photons. A photon is a particle of radiation, but it can also be recognized as a wave. It has zero rest mass, integer spin and no charge. Quantum theory predicts that a photon in vacuum with frequency ν, or wavelenght λ carries the energy

$$E_f = h\nu = \frac{hc}{\lambda}, \tag{2.2}$$

where h is Planck's constant ($h = 6.62607 \cdot 10^{-34}$ Js).

2.2 Blackbody radiation

In 1860 G. Kirchhoff formulated a law, which says

$$F(\lambda, T) = \frac{E}{B}, \tag{2.3}$$

where $F(\lambda, T)$ represents the function of radiation, T is the temperature of a body, E is the emissivity and B is an absorbtion. If a body absorbs all radiation (meaning it does not reflect and it is non-transparent), we call it black. Absolute blackbody is an object, for which $B = 1$, so

$$F(\lambda, T) = E. \tag{2.4}$$

We can see that intensity of an emission depends only on the wavelenght and temperature of the blackbody T. The blackbody is only an ideal model. Stars are not blackbodies, but in first approximation for simplicity we consider them as they were, which is used in stellar photometry.

A lot of scientists were trying to figure out the exact look of the function $F(\lambda, T)$ for a quite long time. Finally Max Planck found out the courageous form of the function, which agreed with experiments

$$F(\lambda, T) = \frac{B}{\lambda^5} \frac{1}{e^{\frac{hc}{kT\lambda}} - 1}, \tag{2.5}$$

where B is a constant, k is Boltzmann's constant. Planck was suprised with the result, because it was not believed that energy could be divided into quanta $h\nu$ (which is Planck's main hypothesis). Later, Albert Einstein used Planck's hypothesis to explain the photoeffect, which brought him Nobel price few years later.

If we integrate function F through all wavelenghts, we get Stefan-Boltzmann's law

$$E = \int_0^\infty F(\lambda, T)\,\mathrm{d}\lambda = \sigma T^4, \tag{2.6}$$

σ is Stefan-Boltzmann's constant. From conditions for maximum of $F(\lambda, T)$ we get Wienn's shifting law

$$\lambda T = k, \tag{2.7}$$

where k stands for Wienn's constant. Planck's and Stefan-Boltzmann's law can be used for determination of temperatures of stars.

2.3 Luminosity and apparent magnitude

Luminosity is the amount of electromagnetic energy which a body (star) radiates per unit of time to its surrounding area. In SI units it is expressed as watts or solar luminosity $L_\odot$ ($L_\odot = 3.846 \cdot 10^{26}$ W). The actual luminosity of the Sun is, however, not exactly equal to $1\,L_\odot$ due to various processes inside the star - the luminisity of the Sun increases and decreases around the value of $L_\odot$.

Flux density is the amount of energy passing per unit of time through unit area perpendicular to the direction of rays in the distance r from the star. Flux density F is expressed in W m^{-2}. As r increases, the area perpendicular to the certain amount of rays increases as well, which leads brightness of the star to decrease. If we can consider stars as point emitters, we can put

$$L = 4\pi r^2 F, \tag{2.8}$$

where F is a flux density and r is distance from the star.

In about 150 B.C., Hipparchus ranked the stars according to their apparent brightness, with 1 representing the brightest stars down to 6 representing the faintest. This corespondes with Weber-Fechner law, which says that stimuli change in geometric series, our eyes, however, percieve them in arithmetic series. Hipparchus wrote down the series of apparent magnitude; the smaller the apparent magnitude is, the brighter the star is. An apparent magnitude m of any star can be determined from Pogson's equation as

$$m = -2.5 \log \frac{j}{j_0}, \tag{2.9}$$

where j_0 is a reference magnitude of the source with $m = 0$ mag. The temperature of a star affects the spectra and the apparent magnitude of the star observed visually and measured in a particular spectral interval. That is why we use bolometric magnitude:

$$m_{bol} = m_v + BC, \tag{2.10}$$

where m_v is an apparent magnitude and BC is bolometric correction. We also put

$$m_{bol} = -2.5 \log \frac{F}{F_0}, \tag{2.11}$$

where $F_0 = 2.553 \cdot 10^{-8}$ Wm^{-2} is a flux density of a source with $m = 0$ mag. The bolometric magnitude of our Sun is -26.821 mag [9]. Since an apparent magnitude depends on a distance, we establish an absolute magnitude M - an apparent magnitude of the star in the distance of 10 pc. By modifications of (2.9) we get the difference between apparent and absolute magnitude called a *distance modulus*:

$$m - M = 5 \log r - 5 = -5 \log \pi - 5, \tag{2.12}$$

where r is a distance in parsecs and $\pi = 1/r$ is a parallax in arcseconds.

2.4 Effective temperature of stars, color index

The surface temperature of the star (our Sun) was first successfully measured after 1879, when Austrian physicist Joseph Stefan found the relation for flux density coming out of the surface of a black body heated to absolute temperature [10]:

$$L = \sigma T_{ef}^4 4\pi R^2, \tag{2.13}$$

where R is the radius of the star, $\sigma = 5.67051 \cdot 10^{-8}\,\mathrm{Wm^{-2}K^{-4}}$ is Stefan-Bolzmann's constant and T_{ef} is the effective temperature. Thus could be determined the effective temperature of solar photosphere (5700 K). However, there was a problem with determining effective temperatures of further objects, because measuring angular radii of distant stars is very inaccurate. It was found out, that the effective temperature may be estimated from spectral analysis (analysing stellar spectra represented by color indices, or location of the maximum of radiation in a spectra and more).

The color index CI is a difference of monochromatic apparent magnitudes of an observed star measured in two different colors c_1 and c_2. For their effective wavelenghts $\lambda_1 < \lambda_2$ we put:

$$CI = m_{c_1} - m_{c_2}. \tag{2.14}$$

The more is the temperature higher, the smaller is its color index. The color index is not only a function of the temperature (it depends on how c_1 and c_2 are chosen), therefore it cannot fully replace it. Since, however, betwen CI and the temperature there is a monotonous relation, we can still partly replace the temperature with the color index, by which we get an estimate of the temperature. We call this temperature *color temperature*. It differs from the effective temperature and is different for different color indices.

2.5 Photometric colors, photometric systems

Bolometric and monochromatic magnitudes are for us, in fact, just an idealization. That is why we measure the brightness of an object in a certain field of wavelenghts. In astronomy photometric systems are set of well-defined passbands (or filters). The sensitivity usualy depends on optical system, detectors or filters used. Photometric systems are usualy represented by width of their passbands:

- broadband - the width of the passband is at least 30 nm (used in Johnson-Morgan UBV system)
- intermediate band - the passband width between 10 and 30 nm
- narrow band - the passband width below 10 nm (we can almost talk about monochromatic radiation)

Naturaly the first used detector was a human eye with its maximum of sensitivity in yellow-green area of spectrum, around 550 nm. Later the magnitudes of stars were measured from photographic plates. After that, measurements became to be made in various colors, the accuracy of these measurements grew. The most widely used photometric system is Johnson UBV system [11], defined by three passbands (filters):

- U (ultraviolet) - sensitivity 300-420 nm, maximum 360 nm
- B (blue) - sensitivity 360-560 nm, maximum 420 nm
- V (visual) - sensitivity 460-740 nm, maximum 535 nm

Later the system was extended to red and infrared due to filters R (red, effective wavelenght 658 nm), I (infrared, effective wavelenght 806 nm), K (2190 nm) and L (3450 nm).

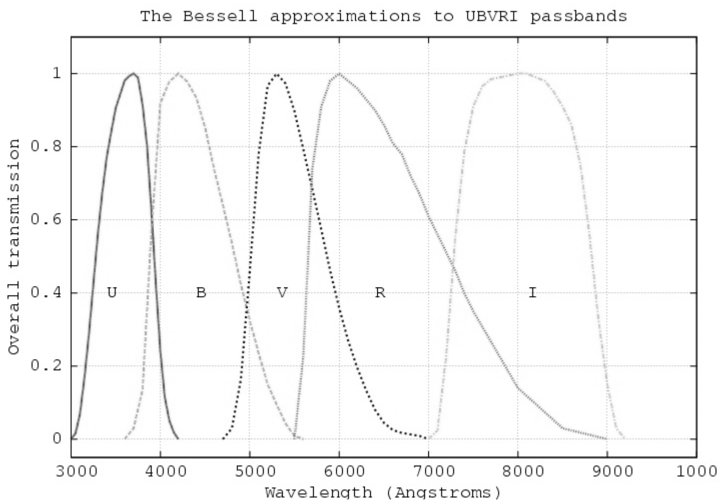

Fig. 2.1: [e3], edited to black and white

The Asiago Database of Photometric Systems keeps around 200 additional photometric systems [e4]. Among others used we should certainly mention Strömgren photometric system (1956), called *uvby photometric system* [12; 13]. Unlike Johnson system, in *uvby* system the height of Balmer jump can be determined. Following Tab. 2.1 shows peak wavelenghts and half-widths of *uvby* photometric system.

Tab. 2.1 Peak wavelenghts and half-widths of *uvby* photometric system [e5]

Filter	u	v	b	y
Peak wavelenght [nm]	350	411	457	567
Half-width [nm]	30	19	18	23

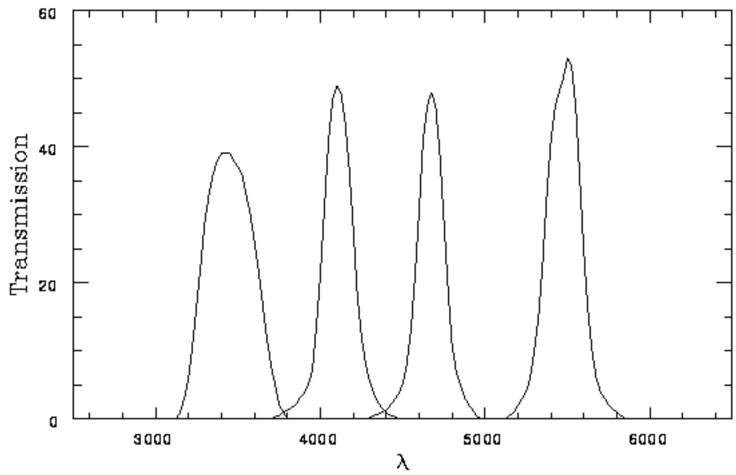

Fig. 2.2: Transmission curves for *uvby* system [e6].

2.6 Reduction of measured magnitudes

The illumination if our CCD detector does not entirely match distribution of a star magnitude, because the impinging radiation is being transformed in two ways.

First transformation medium is the atmosphere. In the visual area of light the shorter wavelenght of incoming radiation, the more is this radiation reduced by the atmosphere. This effect is called the atmospheric extinction and it is the result of absorbtion and scattering of the incoming radiation. An extinction coefficient in current colour represents percent of attenuation of incoming light in magnitudes after passing through a layer of atmospehere with star observed in zenith. Therefore we consider radiated unit column of air masses. It has been found that a column of air masses X is inversely proportional to cosinus of zenith distance z. In real life, following approximate pattern works well [14]:

$$X = (1 - 0.0012 \tan^2 z) sec\, z \tag{2.15}$$

More accurate pattern was deduced by Bemporad [14]:

$$X = \sec\, z - 0.0018167Q - 0.02875Q^2 - 0.0008083Q^3, \tag{2.16}$$

where $Q = \sec\, z - 1$. For measured magnitude m we can write

$$m = m_0 + kX, \tag{2.17}$$

where k is linear extinction coefficient, m_0 is a magnitude measured outside the atmosphere.

The second transformation medium is our detector itself. However, this issue is out of scape of this thesis.

Chapter 3

HR diagram

Hertzsprung-Russell diagram or HR diagram describes relations between stars' absolute magnitudes or luminosities versus their spectral types and effective temperatures.

3.1 The history of HR diagram

In the beginning of 20th century a few distances of several closest stars had been already known from measurements by trigonomical parallax. This information about a distance was key, because without knowing a distance, relative quantities could not be transfered into absolute quantities. After several decades, a few parallax of several stars were available, which led scientists to think about relations between absolute quantities and directly measureable characteristics related to effective temperature.

Most of astrophysicists of 19th century believed that spectral sequence *O-B-A-F-G-K-M* is an evolutional sequence, meaning a star during its evolution goes through each of those phases - the star would contract, get smaller, weaker and colder. For example red stars would have to be small and have a low luminosity. However, in 1905 it was found out that several red stars are very distant, so their luminosity must be high [15]. In 1910 Hans Rosenberg plotted the dependence of apparent magnitude on spectral classification of several stars from Pleiades [16]. Although he did not use the absolute magnitude, due to the fact that all members of Pleiades are in the same distance, it was clear the apparent magnitude would differ from absolute only by a constant distance modulus. In this first HR diagram a diagonal line called *main sequence* was evident, there were, however, sizeable and relatively cold stars not in the group of main sequence stars.

First HR diagram as we know it today (the relation between an absolute magnitude and spectral type) introduced in 1913 H. N. Russel [17]. He approved Hertzsprung's and Rosenberg's conclusions and made a new nomenclature - big cold objects he called *giants* and small stars he called *dwarves.*

Later, another question came up: can be determined from a stellar spectra where to put it in HR diagram? W. S. Adams and A. Kohlschütter studied the spectra of giants and dwarves. It showed up, that the difference of spectra is related to density and pressure in giants' and dwarves' photosphere (this is the principle of Morgan-Keenan spectral classification [18]). Lines of ionised metals are in giants' spectra strengthened, on the other hand, due to very frequent collisions the spectral line of dwarves are extended. Thanks to this information astronomers could place a star into the area of HR diagram and determine its absolute magnitude and then its distance. This procedure is called *the method of spectroscopic parallax*. One disadvantage is the inaccuracy of determining of the absolute magnitude.

In 1924 Arthur S. Eddington predicted the existence of relation between the mass of a star and its luminosity [19]. Thanks to the mass calculated from the measurement of binary stars, masses of more stars could be plotted in HR diagram. Eddington's prediction was confirmed - it appeared it could be applied for main sequence stars, however, the structure of giants is much more complicated. R. J. Trumpler got to conclusion that there are differences between masses of stars in cluster of various types. The astrophysics eventually came to conception of gradual evolution from main sequence stars all the way to the giants area, which means that many open clusters are being relatively young inhabitants of our Galaxy. In 1957 A. R. Sandage pointed to another fact: if we construct a summary HR diagram for greater number of clusters, we can, on the basis of deflection of the cluster from main sequence, determine its relative age.

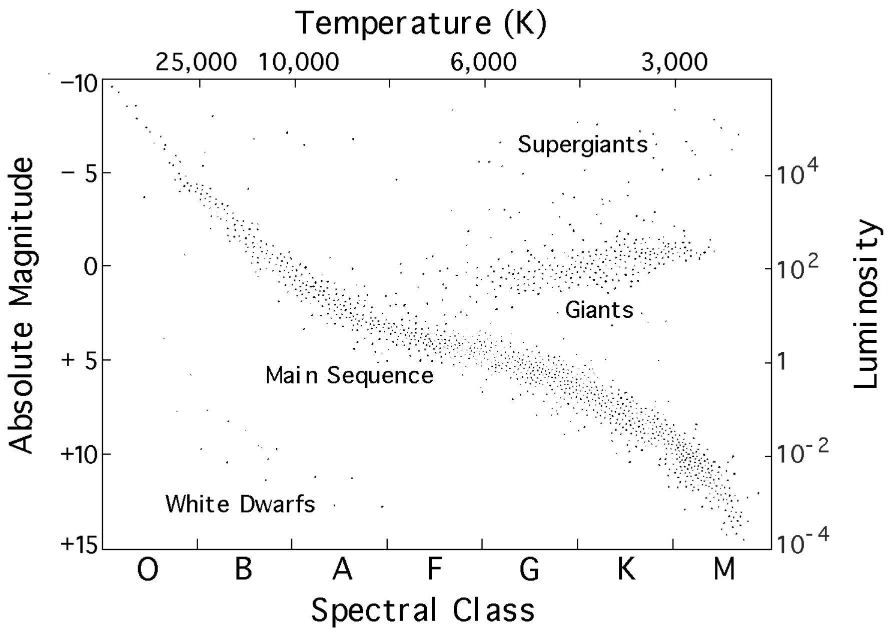

Fig. 3.1: HR diagram [e7]. On the vertical axis we plot and absolute magnitude or luminosity, on the horizontal axis we plot a spectral type or an effective temperature. HR diagram is not equally filled. Notice groups of main sequence stars, supergiants, giants and white dwarves. The structure of main sequence stars is not complicated, on the other hand the structures of giants nad supergiants are very complicated. 90 % of our closest stars are located on the line of main sequence.

3.2 HR diagram of open clusters

Colour-magnitude diagram (CMD) is based on HR diagram - practically it is a HR diagram for open clusters. If we plot main sequence stars of same age but various mass, we will find out that the more is open cluster older, the more is the line of main sequence curved to the area of red giants. The distribution of stars from open clusters is different from distribution in an ordinary HR diagram. Open clusters have their sequences very obvious and sharply defined - we can fit them with a continuous curve - although sometimes the curve may be interrupted.

Soon after the birth of an open cluster, all stars take position on zero age main sequence and they keep evolving. Stars with greater mass evole faster and take position closer to the area of red giants towards greater luminosity but lower temperature making a twisted curve in main sequence, while low mass stars stay in their zero age main sequence. An isochrone is a curve connecting stars of the same age but different mass. A turning point is the place when the isochrone is significantly bended. Through time the turning point shifts down to the areas with lower masses. The location of the turning point helps to determine the age of an open cluster. CMDs of various cluster differ from each other due to different ages of their stars.

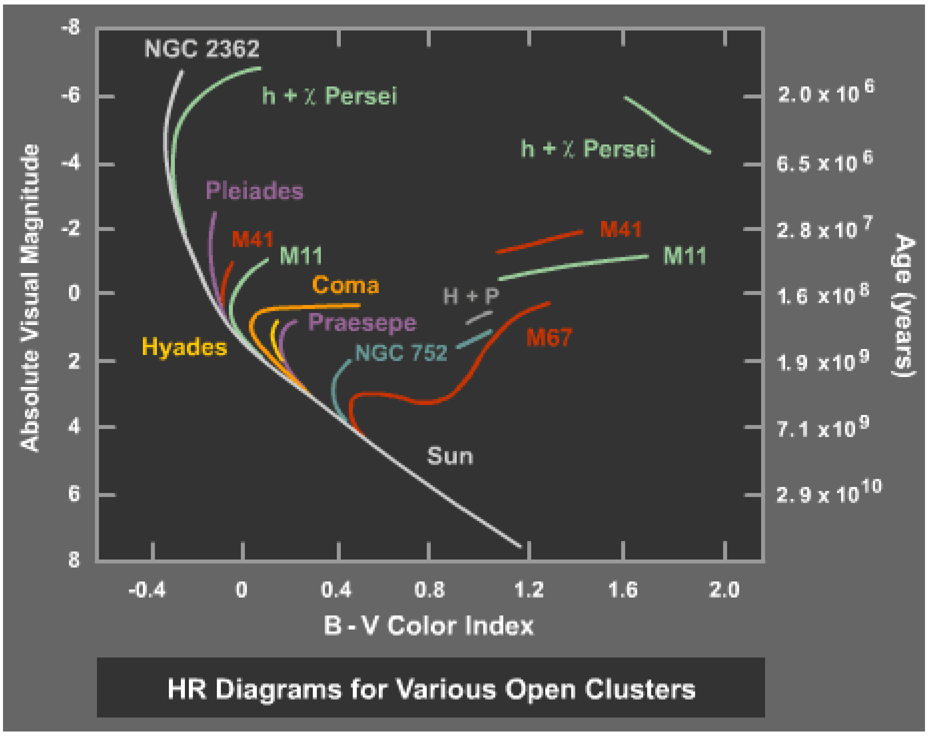

Fig. 3.2: [e8]

Chapter 4

CCD photometry

Charged coupled device (CCD) is an electronic component used for recording the stationary and moving images. In engeneering there are plenty of uses, for example videocameras, digital cameras, faxes, barcode readers, scanners and finally in astronomy as detectors. This technology was invented by W. Boyle and G. E. Smith in 1969. In 2009 they both were awarded the Nobel Prize for Physics [e9].

4.1 How CCD works

CCD uses the photoeffect, when a photon of light excites an electron. The electron is trapped in a potential well, by which it cumulates the charge. Each of these potential wells represents one pixel of CCD sensor.

In the beginning of the process the CCD sensor is without any access to light. The sensor is removed all its free electrons, which leads to deleting any previous information. During an exposition impacting photons excite electrons in a semiconductor and these are attracted by positively charged electrodes. Excited electrons leave the holes behind, which interact with negative electrodes. In next phase the huddles of electrons from each pixel are attracted to electrodes and then led to an output amplifier, which will amplify the low current coresponding with the number of caught electrons to stronger signal, proper for further processing.

Data from CCD camera are saved in FITS format (an universal astronomical format, which gives an information about frames, spectra or data tables). Basic version of FITS format contains two parts. First is a head, which carries among others the information about image size, exposition (start and duration) or which filter was used during capturing. The second folder is data (the image itself). Data are put in table, the values of pixels are proportional to impact radiation.

4.2 The correction of CCD frames

A simple CCD image is often visualy not attractive due to effects in camera, such as the therma and readoutl noise and divergent sensitivity of pixels to light (caused for example by a dust on the chip). Data gained from the image without making a correction may lead to significant deviation from the correct result. Correction frames bias, dark frame and flat field are taken during the observation.

4.2.1 Dark frame and bias

Dark frame captures the influence of the thermal noise. The signal in detector does not corespond only with the image we are capturing, but also with the thermal noise inside the device. Most of cameras are cooled, the effect, however, cannot be omitted completely. The dark frame is captured like any other frame, however, this time with he shutter closed. The exposition time of our dark frame should be the same as an exposition time of the frames we would like to correct. We can also capture bias, which is dark frame with infinitely short exposition time (the shortest possible). Correction itself to bias or dark frame is simply a differ of those frames. For final processing we use averaged master dark frame or master bias.

4.2.2 Flat field

Pixels inside the CCD detector are differently sensitive to light. In addition to this, there might be dust on the surface of the chip. Flat field is a frame of evenly illuminated area. Because of flat field, we now have a certain standard of how are different pixels differently sensitive and we can make a correction. The corrected frame is just a division of the origin frame (corrected for dark and bias) and normalised flat field.

Chapter 5

Practical part

The purpose of this bachelor thesis is to determine basic characteristics of open clusers Chupina 1, Chupina 2 and Messier 67 - their distances and ages. I used data measured by myself in Masaryk university observatory in Brno.

5.1 Measured data

All of three open clusters are located in Cancer constellation, the coordinates of their centers are [e10; e11; e12]:

$$\text{Chupina 1} : \alpha = +8^h\,50.1^m,\ \delta = +11^\circ\,56'\,7'',$$

$$\text{Chupina 2} : \alpha = +8^h\,50.5^m,\ \delta = +12^\circ\,17'\,7'',$$

$$\text{Messier 67 (NGC 2682)} : \alpha = +8^h\,51.3^m,\ \delta = +11^\circ\,48'.$$

All data come only from one-night observation in Brno, Kraví hora on 3.2.2014, used telescope is a reflector 620/2780 mm, newtonian type, with CCD camera G2-4000 of company Moravské přístroje. Frames were taken in Strömgren filters v, b, y. The exposure times of dark frames are 60 s for filter y, 70 s for b and 100 s for filter v. Due to the fact that all data were taken in one night, there are only few frames of open clusters corresponding to each filter: 6 frames of Chupina 1, 4 frames of Chupina 2 and 11 frames per filter belonging to M 67.

Messier 67 is a well-known open cluster, that is why I decided to process data from M 67 first, compare them with actual results and then apply same editing processes and calculations to Chupina 1 and Chupina 2. Obtained data in FITS format were edited by software *Munipack* [e13], from which I gained by aperture photometry averaged dark frames, flat fields and instrumental magnitudes as well.

5.2 Messier 67

Messier 67 (or NGC 2682) is located outside the galactic disc, thus most of the stars captured in frames belong to Messier 67.

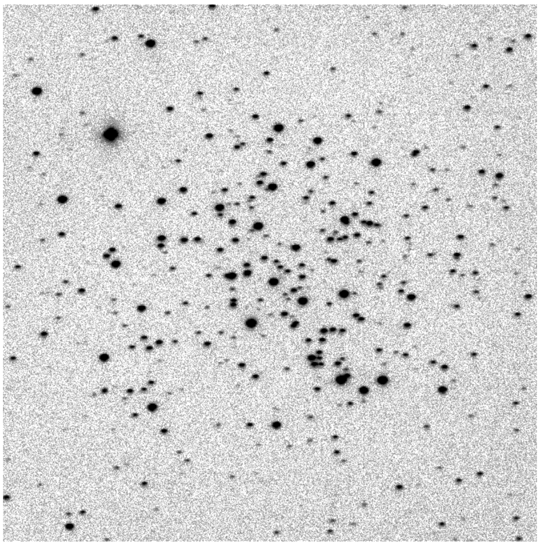

Fig. 5.1: CCD image of Messier 67 in filter y.

As we can see, stars in Fig. 5.1. are blurred and even after dark frame and flat field correction there is still strong background noise.

5.2.1 Photometric calibrations, the age and distance

To get apparent magnitudes from our instrumental magnitudes, we first must find calibration coefficients, which transfer instrumental magnitudes to apparent magnitudes. As a standard star with known magnitudes in vby filters I chose stars from the same open cluster I was studying (Messier 67), because of the great amount of data avaiable. I found few stars in records of vby observations and used them as standards [20]. In Tab. 5.1 there is a list of standard stars used for calibration. Indices indicate which filter is used (capital letters are used for differentiation between standard magnitudes and instrumental magnitudes shown in calibration formulas).

Tab. 5.1: Positions and magnitudes of used standard stars.

Star No.	α [h m s]	δ [° ′]	m_V [mag]	m_B [mag]	m_Y [mag]
1	08 49 08	+12 00.6	10.96	10.618	10.496
2	08 48 55	+12 01.4	12.26	11.749	11.362
3	08 48 34	+11 54.7	13.443	12.903	12.532
4	08 48 17	+12 01.4	12.732	12.055	11.588
5	08 48 19	+11 57.1	12.66	12.086	11.69
6	08 48 19	+11 56.3	11.332	10.94	10.763

We fit linearly instrumental magnitudes v, b, y as functions of standard magnitudes m_V, m_B, m_Y and obtained calibration coefficients:

$$v - b = (0.5 \pm 0.03) + (1.05 \pm 0.05)(m_V - m_B), \tag{5.1}$$

$$b - y = (-0.22 \pm 0.01) + (1.00 \pm 0.03)(m_B - m_Y), \tag{5.2}$$

$$b - m_B = (4.66 \pm 0.02) + (2.13 \pm 0.06)(m_B - m_Y), \tag{5.3}$$

$$y - m_Y = (4.88 \pm 0.02) + (2.13 \pm 0.04)(m_B - m_Y). \tag{5.4}$$

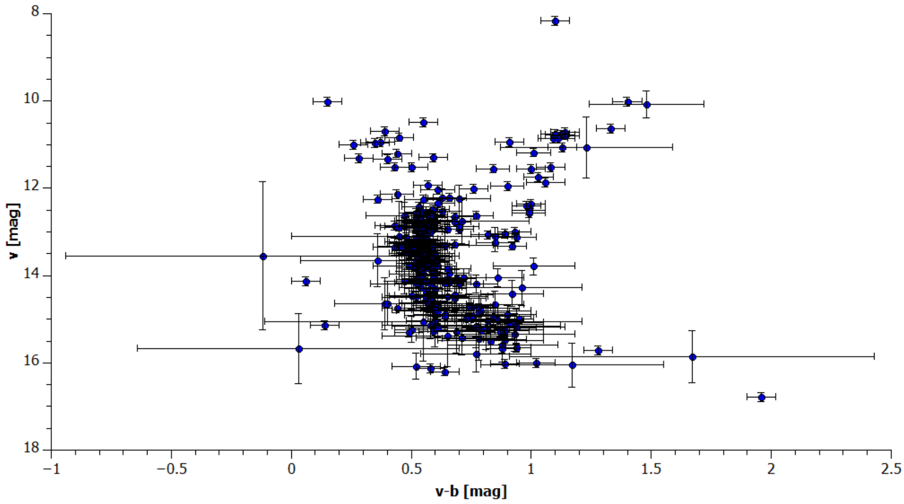

Fig. 5.2: $v - b$ diagram of Messier 67.

As mentioned in section 3.2, from the shape of colour-magnitude diagram some of paramaters of studied open cluster can be determined. The age and distance can be obtained by fitting data with theoretical continuous curve - an isochrone. On Fig. 5.2 there is $v - b$ diagram and on Fig. 5.3 a $b - y$ diagram fitted with a theoretical isochrone. Unfortunately, experimental data in $v - b$ diagram show no turning point (figures are $b - y$ diagrams; $v - b$ diagrams of M 67, Chupina 1 and Chupina 2 are available in *Appendix*), they fit to the theoretical isochrone only in relatively small area. On Fig. 5.4 in blue colours there are stars that fit to the isochrone. The list of theoretical isochrones published Clem et al. [21]. The best fit gives an isochrone with $Y = 1.938$, $Z = 0.2478$ and cluster age 4 Gyr. By shifting the isochrone to the area of experimental data where it fits most precisely, I got distance modulus (9.5 ± 0.3) mag and the distance of Messier 67:

$$r = (787 \pm 108)\,\mathrm{pc}. \tag{5.5}$$

The actual age of Messier 67 published by Harvey et. al. is 4 Gyr [22] and on the online portal WEBDA is published its distance, r= 908 pc [e14]. My result is affected by relatively big deflection 108 pc. The reason might be the low quality of CCD frames caused by light pollution and maybe by the CCD camera, but most probably the fitting of the isochrone was imprecise because of a low number of standard stars used for photometric calibration.

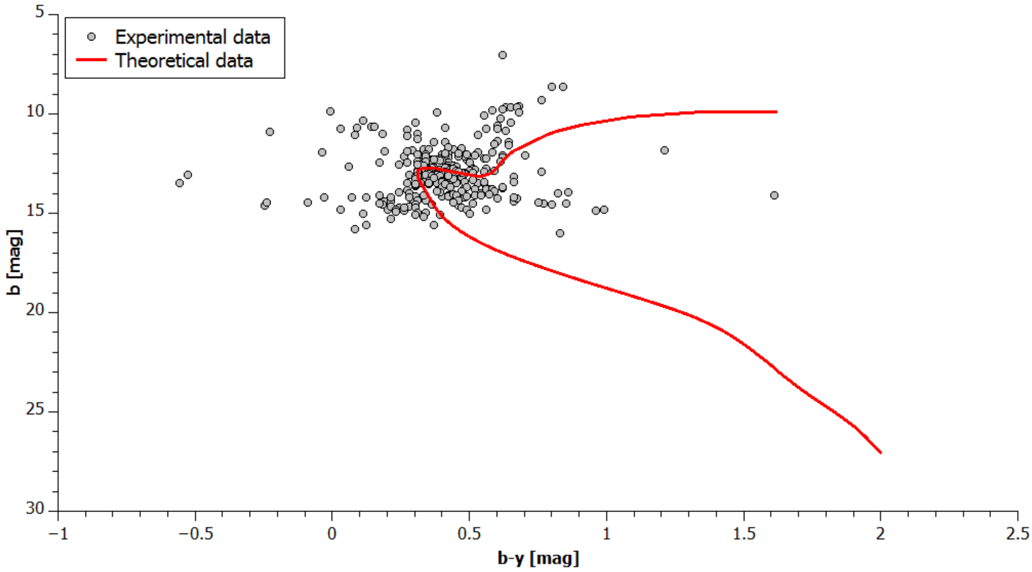

Fig. 5.3: $b-y$ diagram fitted with a theoretical isochrone.

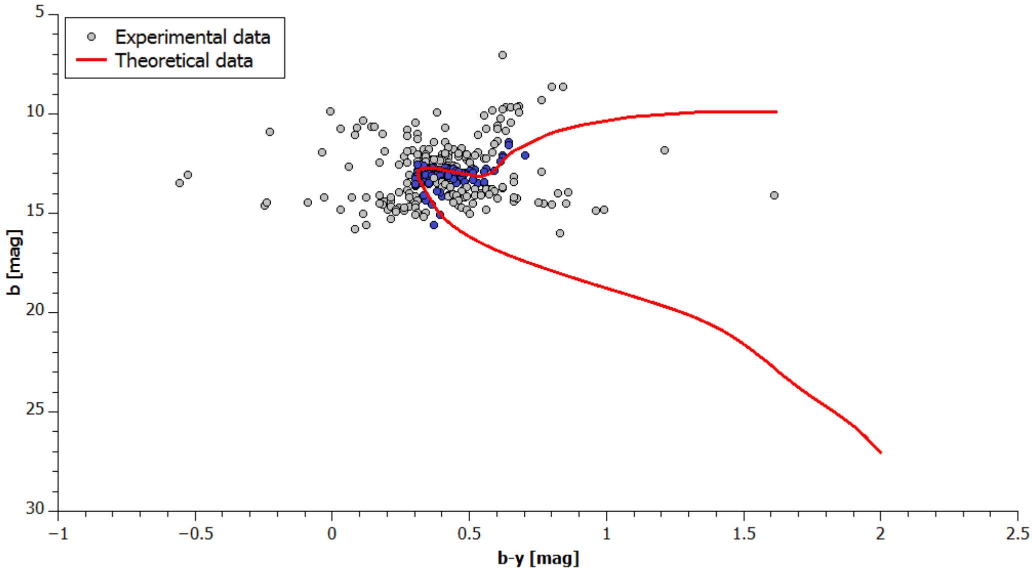

Fig. 5.4: $b-y$ diagram fitted with a theoretical isochrone. Experimental data which copy the shape of isochrone are blue.

5.3 Chupina 1

Chupina 1 is not very numerous open cluster. Membership probabilities of Chupina 1 and also Chupina 2 are published in [23]. As obvious from Fig. 5.5, our CCD images are blurred. After photometric corrections I used formulas (5.1)-(5.4) to transfer instrumental magnitudes to apparent magnitudes.

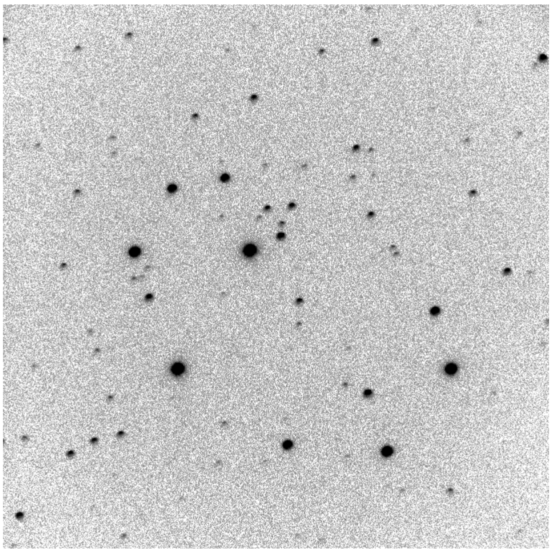

Fig. 5.5: CCD image of Chupina 1.

On Fig. 5.6 is plotted $v - b$ diagram, on Fig. 5.7 there is a $b - y$ diagram with a theoretical isochrone found in [21]. The best fit gives an isochrone with $Y = 1.938$, $Z = 0.2478$ and cluster age 3 Gyr. It is very hard to find stars which copy the shape of the isochrone, due to very low number of stars and measured data. Stars which fit most precisely are shown on Fig. 5.8 as blue.

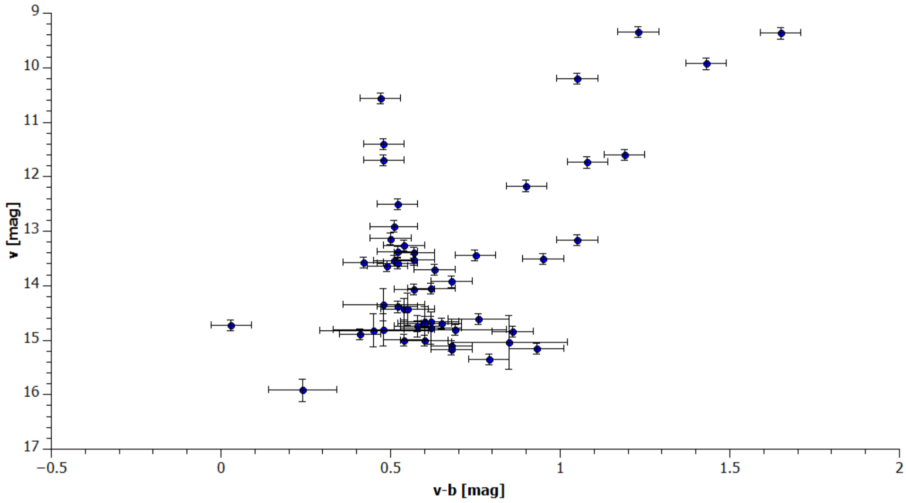

Fig. 5.6: $v - b$ diagram of Chupina 1.

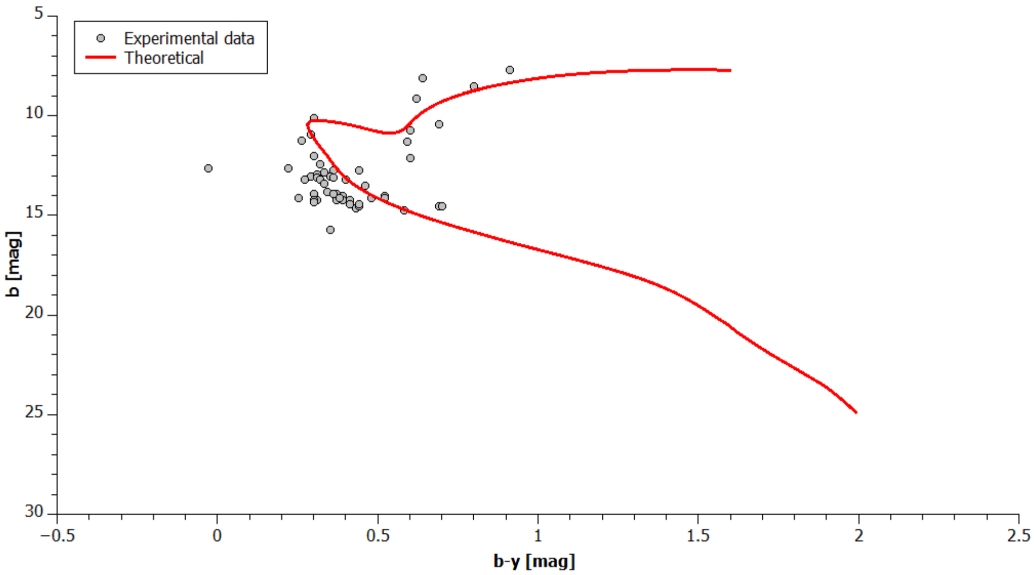

Fig. 5.7: $b - y$ diagram of Chupina 1 fitted with a theoretical isochrone.

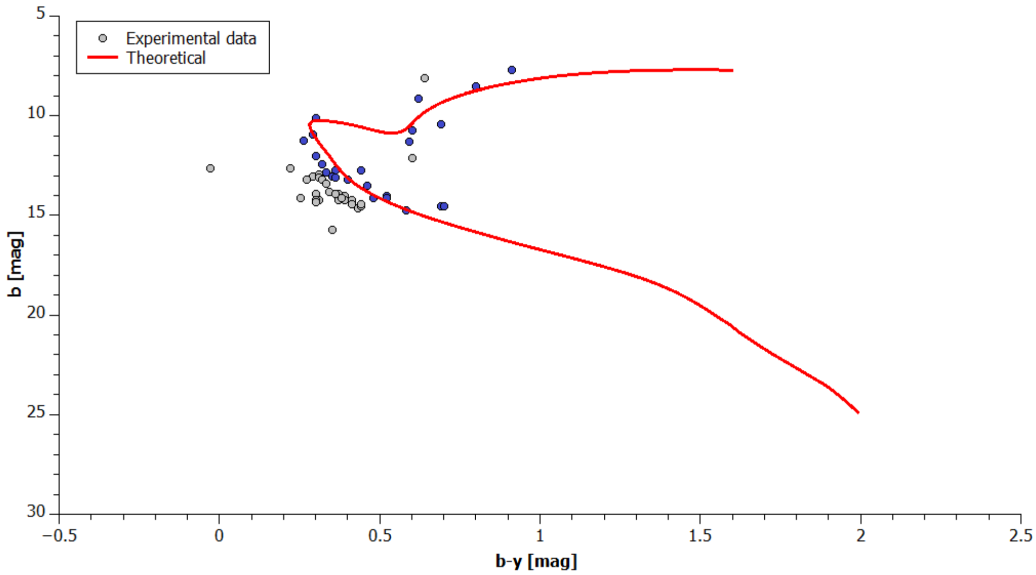

Fig. 5.8: $b-y$ diagram of Chupina 1 fitted with a theoretical isochrone. Experimental data which copy the shape of isochrone are blue.

By shifting the isochrone I obtained a distance modulus (8.2 ± 0.5) mag and the distance of Chupina 1:

$$r = (436 \pm 89)\,\text{pc}. \tag{5.6}$$

There are no references about age or distance of Chupina 1, but I used same methods as with Messier 67 and the frames were blurred as well. Therefore we can expect same deflection as it was with Messier 67. Estimated age of Chupina 1 is 3 Gyr and its distance, $r = (436 \pm 89)$pc.

5.4 Chupina 2

Open cluster Chupina 2 is very similiar to Chupina 1 by its shape and number of stars. Fig. 5.9 shows a CCD image of Chupina 2, which is blurred.

As previously, I used calibration formulas (5.1)-(5.4) and the list of isochrones from Clem et al. [21]. The best fit gives an isochrone with $Y = 1.938$, $Z = 0.2478$ and cluster age $2,5$ Gyr. On Fig. 5.10 there is a $v-b$ diagram, on Fig. 5.11 a $b-y$ diagram with experimental data and the theoretical isochrone. Due to very low number of stars and measured data, there only a few stars that fit with the isochrone. Stars which fit to the isochrone most precisely are blue in Fig. 5.12.

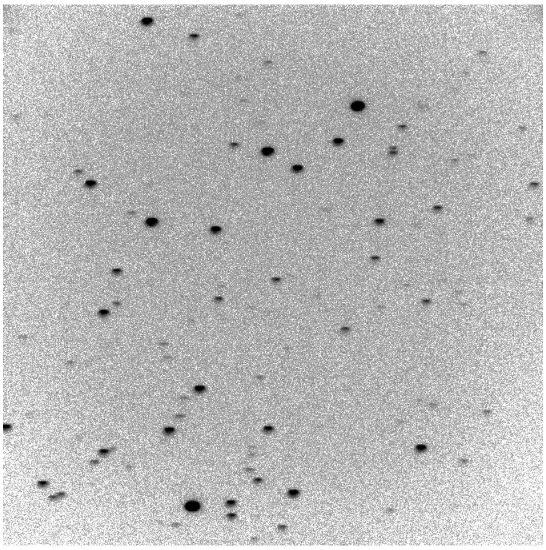

Fig. 5.9: CCD image of Chupina 2.

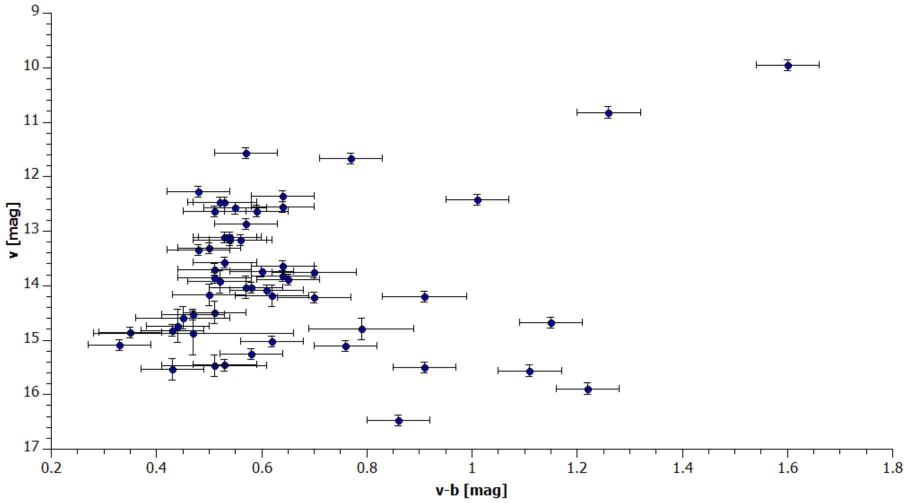

Fig. 5.10: $v - b$ diagram of Chupina 2.

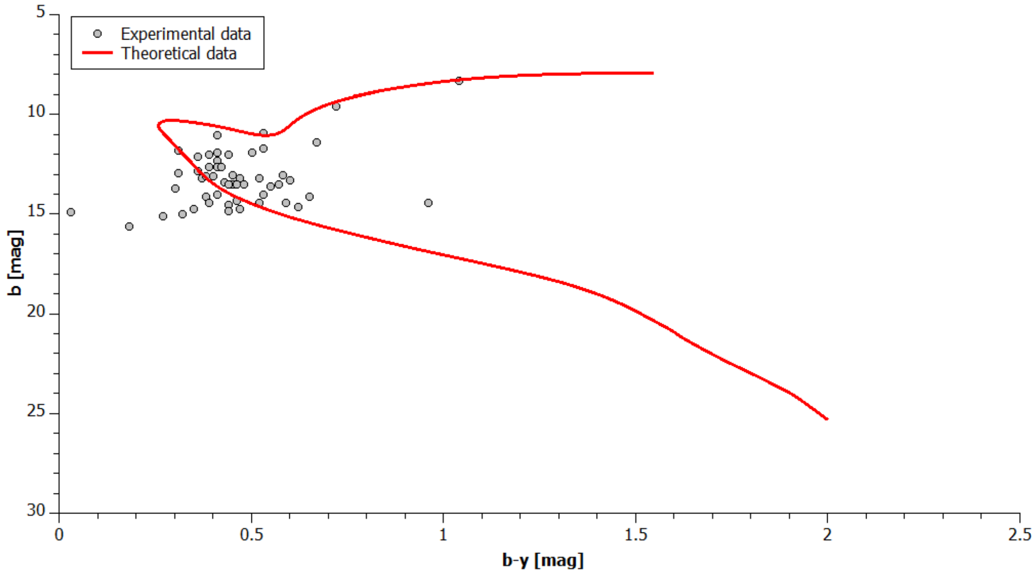

Fig. 5.11: $b - y$ diagram of Chupina 2 fitted with a theoretical isochrone.

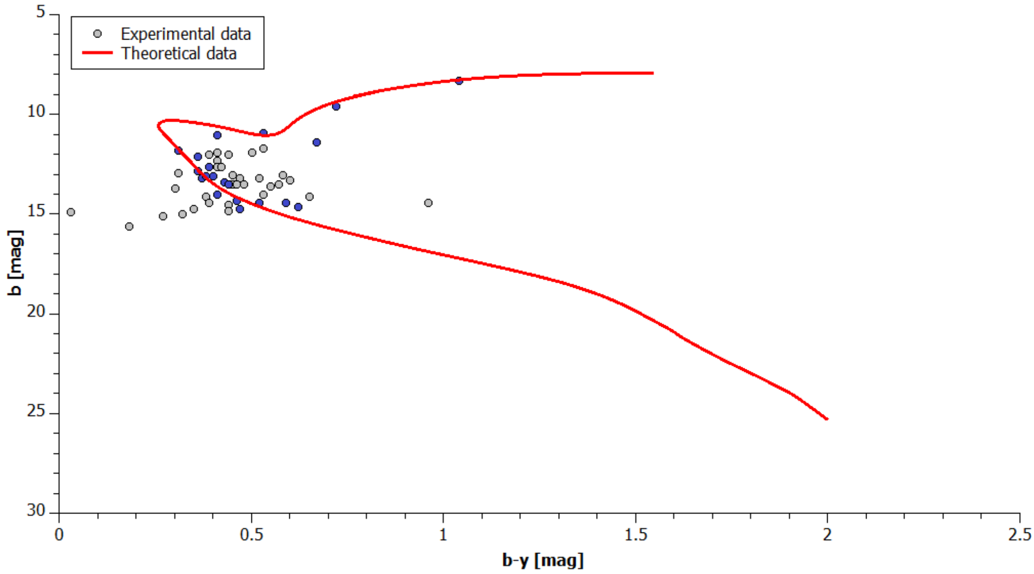

Fig. 5.12: $b-y$ diagram of Chupina 2 fitted with a theoretical isochrone. Experimental data which copy the shape of isochrone are blue.

The distance modulus obtained by shifting the isochrone is (8 ± 1) mag and the distance of Chupina 2:

$$r = (412 \pm 177)\,\mathrm{pc}. \tag{5.7}$$

As mentioned previously, there are no references of Chupina 1 or Chupina 2 to check my results. Taking into account the amount of data and the quality of CCD frames, the result distance of Chupina 2 ($r = 412 \pm 177$ pc) and its age 2.5 Gyr can be considered only as an estimate.

5.5 Belonging to open clusters

The angular distances of Chupina 1 and Chupina 2 from Messier 67 are relatively small (Fig. 5.13). Gained results show a suspicion that Chupina 1 and Chupina 2 are not open cluster, but just groups of stars located on the edge of Messier 67 - meaning that Chupina 1 and Chupina 2 would be parts of open cluster Messier 67.

On Fig. 5.14 and Fig. 5.15 there are plotted obtained magnitudes from all three open clusters into one colour-magnitude diagram. The fact, that all three open clusters are located in similiar positions on vertical axis, is very suspicious. If Chupina 1, Chupina 2 and Messier 67 were three separated open clusters, considering small angular distances between them they would have different distance modulus and they would differ in location on the vertical axis.

To be sure about this conclusion we would have to make an analysis of movements in open clusters and spectroscopy. Since we did not make these steps and because of the quality and quantity of our data, we cannot proclaim that Chupina 1 and Chupina 2 are not open clusters separated from Messier 67.

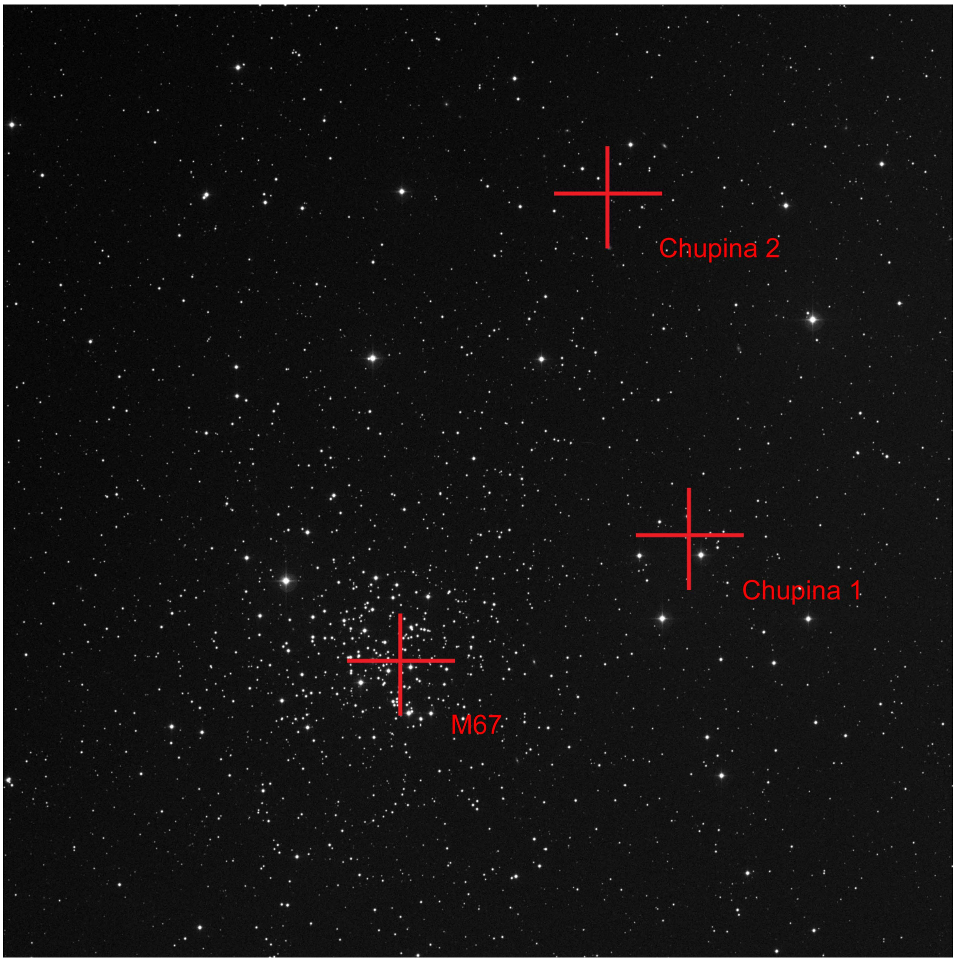

Fig. 5.13: The view on studied open clusters Chupina 1, Chupina 2 and Messier 67. The picture was taken from [e15]. Description was added.

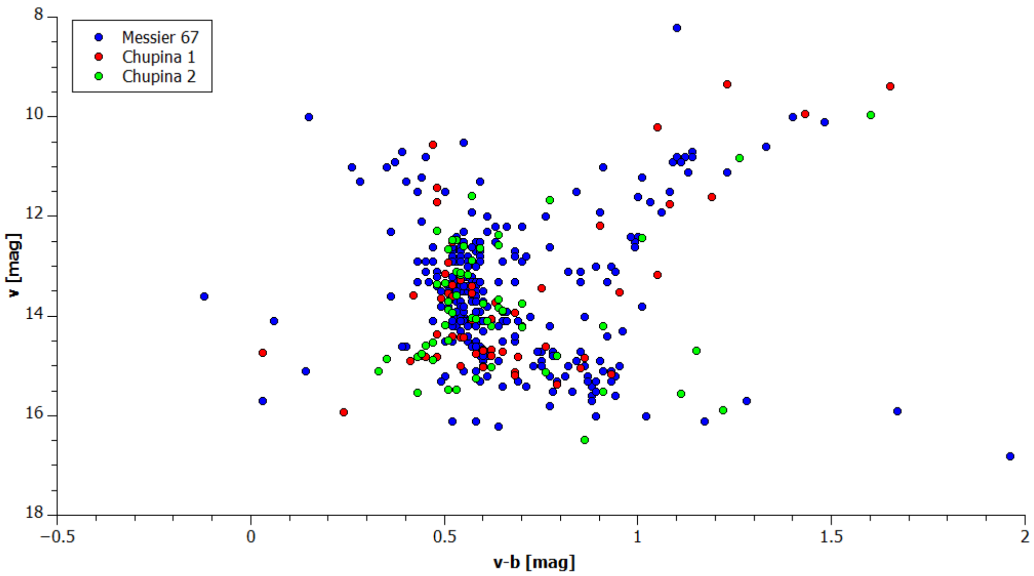

Fig. 5.14: $v - b$ diagram of three studied open clusters.

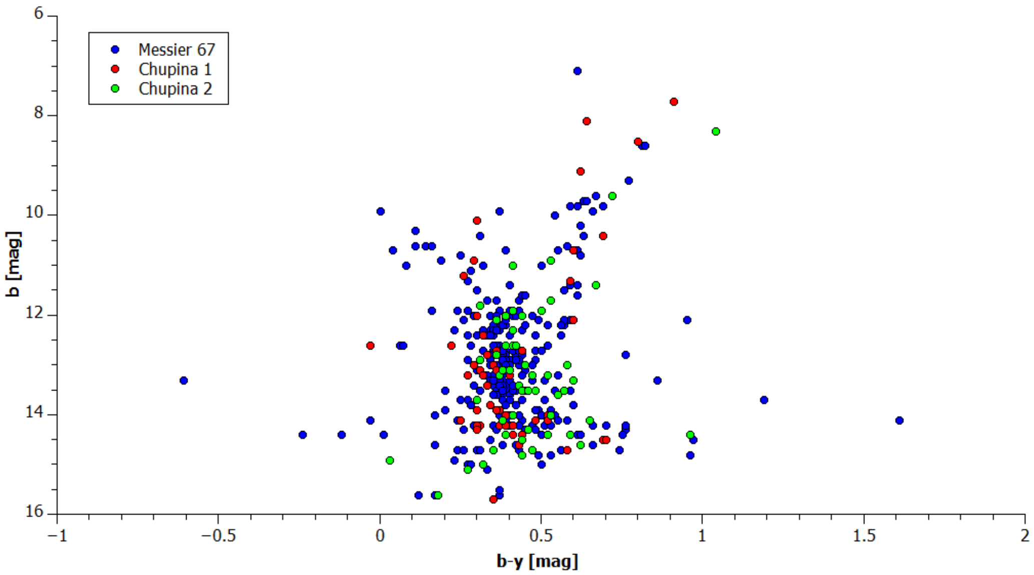

Fig. 5.15: $b - y$ diagram of three studied open clusters.

Conslusion

For selected open clusters with unknown parameters Chupina 1 and Chupina 2 and for a reference open cluster Messier 67 photometric measurements in colours *vby* were obtained on Masaryk university observatory. The measurement was realized with reflector 620/2780 mm, newtonian type, CCD camera G2-4000 of comapany Moravské přístroje on 3.2.2014. The correction of dark frames and flat fields as well as an aperture photometry was executed with software *Munipack* [e13], which provided instrumental magnitudes of all three open clusters.

Measured colour-magnitude diagrams were compared with theoretical models of isochrones taken from [21]. With the isochrones that fitted best with colour-magnitude diagrams I was able to determine the age and distance of selected open clusters.

The age of Messier 67 was determined to 4 Gyr, which matches with actual result publicated in [22] and obtained distance, from my measurements (787 ± 108) pc, is very close (considering the deviation) to the value publicated by WEBDA (908 pc) as well. The reason of such big deviation is most probably the low amount of measured data, which caused that in $v - b$ and $b - y$ diagrams was too few stars to recognise the turning point precisely.

Chupina 1 and Chupina 2 had too few stars and because of only few CCD frames, the turning point was not obvious in $v - b$ and $b - y$ digrams. The age of Chupina 1, resp. Chupina 2 was determined to 3 Gyr, resp. 2.5 Gyr and their calculated distances (436 ± 89) pc for Chupina 1 and (412 ± 177) pc for Chupina 2. No references of ages or distances of Chupina 1 and Chupina 2 were found. Considering the deviation of results for Messier 67, the results for Chupina 1 and Chupina 2 can be considered only as estimates.

Due to the fact that angular distances of Chupina 1 and Chupina 2 from Messier 67 are relatively small, it was important to rethink, whether Chupina 1 and Chupina 2 are really open clusters or just groups of stars belonging to Messier 67 located on the edge of M 67. To make such conclusions, we would have to make the analysis of the motions in open clusters and spectroscopy. Considering this fact and the quality and quantity of our data, we cannot proclaim that Chupina 1 and Chupina 2 are parts of open cluster Messier 67.

CCD frames were highly blurred, the stars on CCD images were not sharp and background noise was significant because of light pollution. Only a little amount of data were obtained. If we had more data and measurements were carried out during darker night and we could ensure the quality of CCD images, the results might be more accurate.

Appendix

5.6 v-b diagrams

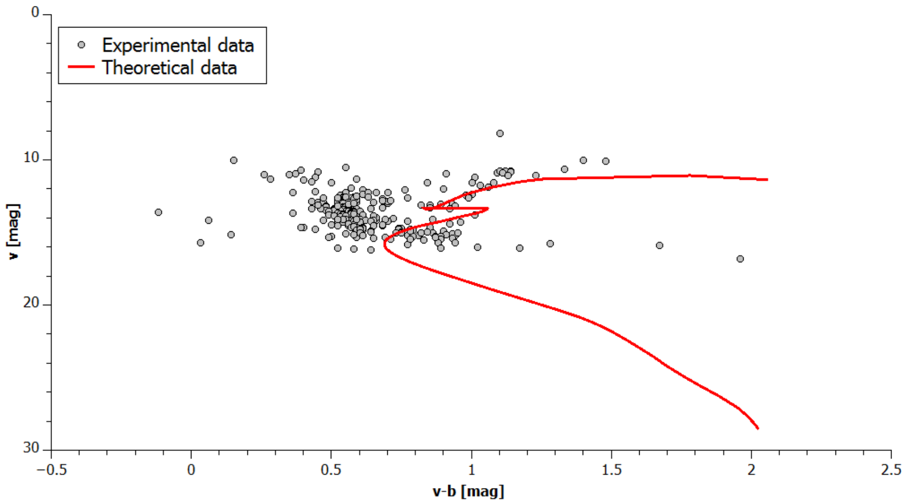

Fig. 5.16: $v - b$ diagram of Messier 67 fitted with a theoretical isochrone.

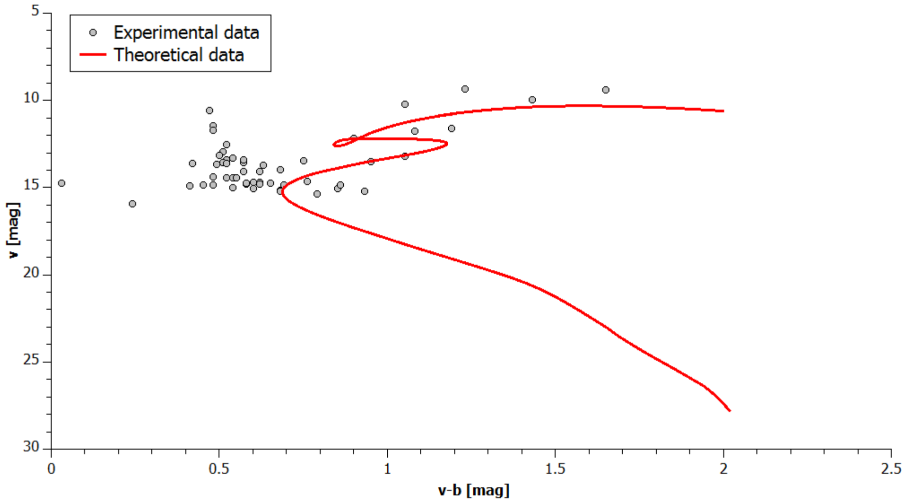

Fig. 5.17: $v - b$ diagram of Chupina 1 fitted with a theoretical isochrone.

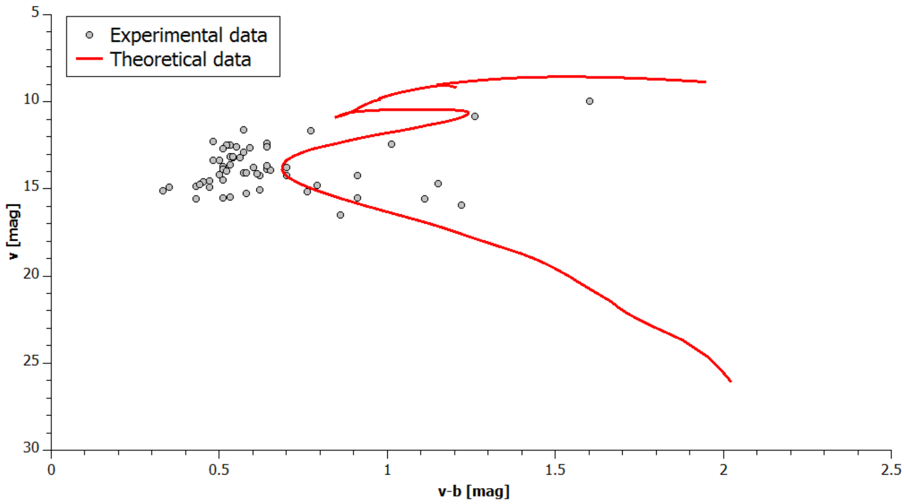

Fig. 5.18: $v - b$ diagram of Chupina 2 fitted with a theoretical isochrone.

5.7 Tables and results of photometry

Used symbols:
No. - star number
α $[^{h\ m\ s}]$ - right ascension
δ $[^{\circ}\ '\ '']$ - declination
m_b [mag] - apparent magnitude in filter b,
m_v [mag] - apparent magnitude in filter v,
m_y [mag] - apparent magnitude in filter y,
the same for m_{v-b} and m_{b-y},
σ_b [mag] - deviation of apparent magnitude in filter b,
σ_v [mag] - deviation of apparent magnitude in filter v,
σ_y [mag] - deviation of apparent magnitude in filter y,
σ_{v-b} [mag] - deviation of (m_{v-b}),
σ_{b-y} [mag] - deviation of (m_{b-y}).

5.7.1 Messier 67

Table A1: Results of photometry, Messier 67

No.	α	δ	m_{v-b}	σ_{v-b}	m_{b-y}	σ_{b-y}	m_v	σ_v	m_b	σ_b	m_y	σ_y
1	08 51 49	+11 53 39	1.10	0.06	0.61	0.04	8.2	0.1	7.1	0.1	6.4	0.1
2	08 51 30	+11 47 17	1.40	0.06	0.81	0.04	10.0	0.1	8.6	0.1	7.8	0.1
3	08 51 17	+11 45 23	1.48	0.24	0.82	0.04	10.1	0.3	8.6	0.1	7.8	0.1
4	08 51 17	+11 48 16	1.33	0.06	0.77	0.04	10.6	0.1	9.3	0.1	8.5	0.1
5	08 51 23	+11 48 02	1.14	0.06	0.67	0.04	10.7	0.1	9.6	0.1	8.9	0.1
6	08 51 12	+11 45 22	0.15	0.06	0.00	0.04	10.0	0.1	9.9	0.1	9.9	0.1
7	08 51 60	+11 55 05	1.09	0.06	0.59	0.04	10.9	0.1	9.8	0.1	9.2	0.1
8	08 51 26	+11 53 52	1.10	0.06	0.63	0.04	10.8	0.1	9.7	0.1	9.0	0.1
9	08 51 13	+11 52 42	1.12	0.06	0.64	0.04	10.8	0.1	9.7	0.1	9.0	0.1
10	08 51 44	+11 56 42	1.11	0.07	0.61	0.04	10.9	0.1	9.8	0.1	9.2	0.1
11	08 51 29	+11 50 33	1.14	0.06	0.67	0.04	10.8	0.1	9.6	0.1	9.0	0.1
12	08 51 27	+11 48 40	0.55	0.06	0.37	0.04	10.5	0.1	9.9	0.1	9.6	0.1
13	08 51 44	+11 44 26	1.13	0.06	0.66	0.04	11.1	0.1	9.9	0.1	9.3	0.1
14	08 51 50	+11 46 07	0.91	0.06	0.54	0.04	11.0	0.1	10.0	0.1	9.5	0.1
15	08 51 56	+11 51 26	0.39	0.06	0.11	0.04	10.7	0.1	10.3	0.1	10.2	0.1
16	08 51 17	+11 50 46	1.01	0.07	0.62	0.04	11.2	0.1	10.2	0.1	9.5	0.1
17	08 51 34	+11 51 10	0.35	0.06	0.14	0.04	11.0	0.1	10.6	0.1	10.5	0.1
18	08 51 49	+11 49 16	0.35	0.06	0.11	0.04	11.0	0.1	10.6	0.1	10.5	0.1
19	08 51 42	+11 51 23	1.08	0.06	0.63	0.04	11.5	0.1	10.4	0.1	9.8	0.1
20	08 51 14	+11 45 01	0.45	0.06	0.31	0.04	10.8	0.1	10.4	0.1	10.1	0.1
21	08 51 21	+11 53 26	0.44	0.06	0.25	0.04	11.2	0.1	10.8	0.1	10.5	0.1
22	08 51 27	+11 51 53	0.26	0.06	0.04	0.04	11.0	0.1	10.7	0.1	10.7	0.1
23	08 51 33	+11 48 52	0.37	0.06	0.16	0.04	10.9	0.1	10.6	0.1	10.4	0.1
24	08 51 22	+11 46 06	1.00	0.06	0.58	0.03	11.6	0.1	10.6	0.1	10.0	0.1
25	08 51 22	+11 52 38	0.59	0.06	0.39	0.04	11.3	0.1	10.7	0.1	10.3	0.1
26	08 51 45	+11 47 46	1.03	0.06	0.61	0.04	11.7	0.1	10.7	0.1	10.1	0.1
27	08 51 24	+11 49 49	0.84	0.07	0.55	0.04	11.5	0.1	10.7	0.1	10.2	0.1
28	08 51 04	+11 45 03	0.40	0.06	0.19	0.04	11.3	0.1	10.9	0.1	10.8	0.1
29	08 51 55	+11 40 26	0.50	0.07	0.32	0.04	11.5	0.1	11.0	0.1	10.7	0.1
30	08 51 42	+11 50 08	1.06	0.08	0.62	0.04	11.9	0.1	10.8	0.1	10.2	0.1
31	08 51 26	+11 43 51	0.28	0.06	0.08	0.04	11.3	0.1	11.0	0.1	10.9	0.1
32	08 51 08	+11 48 09	0.43	0.06	0.28	0.04	11.5	0.1	11.1	0.1	10.8	0.1
33	08 51 30	+11 48 58	0.90	0.07	0.50	0.04	11.9	0.1	11.0	0.1	10.5	0.1
34	08 50 56	+11 52 15	0.57	0.06	0.40	0.04	11.9	0.1	11.4	0.1	11.0	0.1
35	08 51 39	+11 51 46	1.00	0.06	0.59	0.04	12.4	0.1	11.4	0.1	10.8	0.1
36	08 51 36	+11 53 35	0.99	0.07	0.57	0.04	12.5	0.1	11.5	0.1	10.9	0.1
37	08 51 20	+11 47 00	0.44	0.07	0.33	0.04	12.1	0.1	11.7	0.1	11.4	0.1
38	08 51 19	+11 58 11	0.98	0.06	0.61	0.04	12.4	0.1	11.4	0.1	10.8	0.1
39	08 51 14	+11 50 38	0.61	0.07	0.40	0.04	12.0	0.1	11.4	0.1	11.0	0.1
40	08 51 39	+11 50 04	0.55	0.08	0.36	0.04	12.3	0.1	11.7	0.1	11.3	0.1

Contd. Table A1: Results of photometry, Messier 67

No.	α	δ	m_{v-b}	σ_{v-b}	m_{b-y}	σ_{b-y}	m_v	σ_v	m_b	σ_b	m_y	σ_y
41	08 51 21	+11 45 53	0.76	0.06	0.27	0.04	12.0	0.1	11.3	0.1	11.0	0.1
42	08 51 08	+11 47 12	0.99	0.07	0.61	0.05	12.6	0.1	11.6	0.1	11.0	0.1
43	08 51 33	+11 50 41	0.36	0.06	0.16	0.04	12.3	0.1	11.9	0.1	11.7	0.1
44	08 51 17	+11 45 29	1.23	0.36	0.69	0.31	11.1	0.7	9.8	0.4	9.1	0.7
45	08 51 43	+11 46 37	0.53	0.07	0.37	0.05	12.4	0.1	11.9	0.1	11.5	0.1
46	08 51 59	+11 46 53	0.54	0.07	0.34	0.04	12.5	0.1	12.0	0.1	11.7	0.1
47	08 51 19	+11 47 03	0.68	0.08	0.47	0.06	12.7	0.1	12.0	0.1	11.5	0.1
48	08 51 19	+11 50 06	0.58	0.07	0.36	0.04	12.6	0.1	12.0	0.1	11.7	0.1
49	08 51 25	+11 47 34	0.54	0.07	0.41	0.06	12.6	0.1	12.0	0.1	11.6	0.2
50	08 51 48	+11 51 12	0.58	0.06	0.40	0.04	12.5	0.1	11.9	0.1	11.5	0.1
51	08 51 07	+11 53 02	0.61	0.07	0.43	0.04	12.3	0.1	11.7	0.1	11.3	0.1
52	08 51 42	+11 49 52	0.77	0.07	0.24	0.05	12.6	0.1	11.9	0.1	11.6	0.1
53	08 51 37	+11 50 05	0.58	0.09	0.39	0.05	12.7	0.2	12.2	0.1	11.8	0.1
54	08 51 32	+11 50 04	0.56	0.08	0.44	0.06	12.8	0.2	12.3	0.1	11.8	0.2
55	08 51 50	+11 49 31	0.59	0.06	0.26	0.03	12.7	0.1	12.1	0.1	11.8	0.1
56	08 51 03	+11 45 47	0.57	0.07	0.42	0.04	12.6	0.1	12.0	0.1	11.6	0.1
57	08 50 52	+11 48 10	0.68	0.06	0.06	0.03	13.3	0.1	12.6	0.1	12.5	0.1
58	08 51 42	+11 43 37	0.52	0.08	0.36	0.04	12.7	0.1	12.2	0.1	11.9	0.1
59	08 51 23	+11 48 49	0.54	0.06	0.36	0.05	12.7	0.1	12.2	0.1	11.8	0.1
60	08 52 04	+11 41 24	0.53	0.06	0.30	0.04	12.9	0.1	12.4	0.1	12.1	0.1
61	08 51 44	+11 46 25	0.70	0.06	0.39	0.04	12.9	0.1	12.2	0.1	11.8	0.1
62	08 51 35	+11 57 57	0.70	0.08	0.45	0.04	12.9	0.1	12.2	0.1	11.7	0.1
63	08 51 53	+11 48 21	0.52	0.06	0.34	0.05	12.8	0.1	12.3	0.1	11.9	0.1
64	08 51 10	+11 41 45	0.68	0.07	0.49	0.05	12.8	0.1	12.1	0.1	11.6	0.1
65	08 50 58	+11 52 22	0.93	0.07	0.59	0.05	13.0	0.1	12.1	0.1	11.5	0.1
66	08 50 52	+11 56 56	0.54	0.08	0.37	0.06	12.8	0.2	12.3	0.1	11.9	0.2
67	08 51 24	+11 47 16	0.63	0.07	0.44	0.06	12.2	0.2	11.6	0.1	11.1	0.2
68	08 51 27	+11 53 27	0.59	0.07	0.35	0.06	12.8	0.1	12.2	0.1	11.9	0.2
69	08 50 54	+11 56 29	0.56	0.06	0.35	0.04	12.9	0.1	12.3	0.1	11.9	0.1
70	08 51 56	+11 50 15	0.94	0.08	0.57	0.05	13.1	0.1	12.2	0.1	11.6	0.1
71	08 51 41	+11 54 29	0.54	0.07	0.32	0.05	12.9	0.1	12.3	0.1	12.0	0.1
72	08 51 20	+11 46 42	0.59	0.06	0.23	0.04	12.9	0.1	12.3	0.1	12.1	0.1
73	08 51 29	+11 45 28	0.89	0.06	0.57	0.05	13.0	0.1	12.1	0.1	11.6	0.1
74	08 51 51	+11 57 50	0.52	0.07	0.32	0.04	12.9	0.1	12.4	0.1	12.1	0.1
75	08 51 15	+11 50 14	0.54	0.07	0.34	0.05	12.9	0.1	12.3	0.1	12.0	0.1
76	08 51 28	+11 52 18	0.54	0.07	0.38	0.05	12.7	0.1	12.2	0.1	11.8	0.1
77	08 51 49	+11 56 51	0.92	0.06	0.48	0.04	13.3	0.1	12.4	0.1	11.9	0.1
78	08 51 24	+11 48 22	0.59	0.06	0.39	0.05	12.7	0.1	12.2	0.1	11.8	0.1
79	08 51 16	+11 52 59	0.54	0.07	0.35	0.04	12.9	0.1	12.4	0.1	12.0	0.1
80	08 51 15	+11 47 24	0.55	0.08	0.29	0.04	12.5	0.2	12.0	0.1	11.7	0.1
81	08 51 18	+11 45 54	0.58	0.07	0.39	0.04	12.7	0.1	12.1	0.1	11.7	0.1
82	08 51 28	+11 49 27	0.45	0.08	0.32	0.04	12.9	0.1	12.4	0.1	12.1	0.1
83	08 51 29	+11 54 14	0.56	0.07	0.36	0.04	12.9	0.1	12.3	0.1	12.0	0.1
84	08 51 60	+11 52 58	0.52	0.06	0.33	0.04	12.9	0.1	12.4	0.1	12.0	0.1
85	08 51 34	+11 49 44	0.47	0.08	0.40	0.06	12.9	0.2	12.4	0.1	12.0	0.2
86	08 51 45	+11 46 46	0.85	0.07	0.56	0.06	13.1	0.2	12.2	0.1	11.7	0.2
87	08 51 47	+11 44 58	0.43	0.08	0.33	0.05	12.9	0.1	12.4	0.1	12.1	0.1
88	08 51 16	+11 50 56	0.82	0.07	0.52	0.05	13.1	0.1	12.2	0.1	11.7	0.2
89	08 51 21	+11 46 16	0.52	0.07	0.34	0.04	12.6	0.1	12.0	0.1	11.7	0.1
90	08 51 19	+11 51 19	0.85	0.08	0.56	0.06	13.3	0.2	12.4	0.1	11.9	0.2
91	08 51 21	+11 45 02	0.56	0.08	0.42	0.07	13.2	0.2	12.7	0.2	12.3	0.2
92	08 51 17	+11 47 01	0.57	0.07	0.37	0.05	13.2	0.1	12.6	0.1	12.2	0.1
93	08 51 44	+11 45 15	0.48	0.08	0.36	0.04	13.1	0.1	12.6	0.1	12.3	0.1
94	08 51 30	+11 43 50	0.53	0.06	0.39	0.04	13.1	0.1	12.6	0.1	12.2	0.1
95	08 51 24	+11 47 10	0.66	0.07	0.45	0.04	12.2	0.1	11.6	0.1	11.1	0.1
96	08 51 32	+11 53 12	0.54	0.06	0.33	0.05	12.9	0.1	12.4	0.1	12.1	0.1
97	08 51 17	+11 50 39	1.01	0.07	0.62	0.04	11.2	0.1	10.2	0.1	9.5	0.1
98	08 51 20	+11 45 52	0.63	0.07	0.27	0.04	12.5	0.1	11.9	0.1	11.6	0.1
99	08 51 17	+11 50 09	0.56	0.07	0.34	0.06	12.9	0.2	12.4	0.1	12.0	0.2
100	08 51 22	+11 46 41	0.52	0.08	0.42	0.06	13.3	0.2	12.8	0.1	12.4	0.2
101	08 52 03	+11 46 04	0.53	0.07	0.35	0.06	13.3	0.2	12.7	0.1	12.4	0.2
102	08 51 21	+11 46 05	0.70	0.13	0.30	0.13	12.2	0.3	11.5	0.2	11.2	0.3
103	08 51 37	+11 54 60	0.54	0.07	0.35	0.05	13.2	0.1	12.6	0.1	12.3	0.1
104	08 51 34	+11 51 45	0.57	0.07	0.41	0.07	13.3	0.2	12.7	0.2	12.3	0.2
105	08 50 59	+11 56 37	0.58	0.07	0.37	0.04	13.3	0.1	12.7	0.1	12.3	0.1
106	08 51 45	+11 41 51	0.52	0.06	0.33	0.04	13.3	0.1	12.8	0.1	12.4	0.1
107	08 50 58	+11 42 12	0.58	0.07	0.43	0.04	13.3	0.1	12.7	0.1	12.2	0.1
108	08 51 26	+11 52 39	0.53	0.08	0.44	0.07	13.3	0.2	12.8	0.1	12.3	0.2
109	08 51 12	+11 46 21	0.54	0.09	0.48	0.06	13.3	0.2	12.7	0.1	12.3	0.2
110	08 51 22	+11 51 29	0.58	0.09	0.34	0.05	13.4	0.2	12.8	0.1	12.4	0.1
111	08 51 25	+11 49 01	0.58	0.07	0.32	0.04	13.3	0.1	12.7	0.1	12.4	0.1
112	08 51 31	+11 48 55	0.90	0.07	0.50	0.04	11.9	0.1	11.0	0.1	10.5	0.1
113	08 51 26	+11 49 09	0.55	0.07	0.28	0.04	13.2	0.1	12.6	0.1	12.4	0.1
114	08 51 28	+11 55 41	0.58	0.07	0.34	0.04	13.4	0.1	12.8	0.1	12.5	0.1
115	08 51 18	+11 42 55	0.52	0.07	0.39	0.05	13.2	0.1	12.7	0.1	12.3	0.1
116	08 51 30	+11 51 30	0.48	0.09	0.35	0.05	13.2	0.2	12.8	0.1	12.4	0.2
117	08 51 06	+11 51 10	0.53	0.07	0.39	0.06	13.3	0.2	12.8	0.1	12.4	0.2
118	08 51 23	+11 49 13	0.43	0.09	0.40	0.07	13.3	0.2	12.9	0.1	12.5	0.2
119	08 51 02	+11 49 01	0.59	0.07	0.41	0.05	13.3	0.1	12.7	0.1	12.3	0.1
120	08 50 53	+11 47 34	0.56	0.08	0.41	0.05	13.2	0.2	12.7	0.1	12.3	0.2

Contd. Table A1: Results of photometry, Messier 67

No.	α	δ	m_{v-b}	σ_{v-b}	m_{b-y}	σ_{b-y}	m_v	σ_v	m_b	σ_b	m_y	σ_y
121	08 51 13	+11 51 40	1.01	0.17	0.76	0.08	13.8	0.2	12.8	0.2	12.0	0.2
122	08 51 53	+11 40 54	0.55	0.07	0.34	0.04	13.5	0.1	12.9	0.1	12.6	0.1
123	08 51 46	+11 44 09	0.52	0.08	0.34	0.07	13.5	0.2	13.0	0.1	12.7	0.2
124	08 50 58	+11 55 15	0.51	0.07	0.38	0.04	13.4	0.1	12.8	0.1	12.5	0.1
125	08 51 14	+11 50 40	0.61	0.07	0.40	0.04	12.0	0.1	11.4	0.1	11.0	0.1
126	08 51 45	+11 45 01	0.56	0.06	0.27	0.04	13.5	0.1	12.9	0.1	12.6	0.1
127	08 52 02	+11 49 08	0.54	0.07	0.34	0.06	13.5	0.2	12.9	0.1	12.6	0.2
128	08 51 09	+11 48 21	0.56	0.07	0.33	0.04	13.4	0.1	12.8	0.1	12.5	0.1
129	08 51 04	+11 40 31	0.54	0.06	0.39	0.05	13.4	0.1	12.9	0.1	12.5	0.2
130	08 51 46	+11 46 27	0.48	0.06	0.37	0.05	13.4	0.1	13.0	0.1	12.6	0.1
131	08 50 59	+11 46 13	0.57	0.07	0.39	0.06	13.5	0.1	12.9	0.1	12.5	0.2
132	08 51 09	+11 46 12	0.55	0.08	0.36	0.06	13.5	0.2	13.0	0.1	12.6	0.2
133	08 51 16	+11 44 33	0.55	0.09	0.43	0.09	13.5	0.2	13.0	0.2	12.5	0.2
134	08 51 50	+11 44 57	0.56	0.07	0.35	0.06	13.0	0.2	12.4	0.1	12.1	0.2
135	08 51 18	+11 43 25	0.51	0.07	0.38	0.05	13.4	0.1	12.9	0.1	12.5	0.1
136	08 51 27	+11 49 20	0.46	0.10	0.43	0.10	13.3	0.2	12.9	0.2	12.4	0.2
137	08 51 01	+11 41 59	0.51	0.07	0.37	0.04	13.5	0.1	13.0	0.1	12.6	0.1
138	08 51 05	+11 45 57	0.55	0.07	0.42	0.04	13.4	0.1	12.9	0.1	12.5	0.1
139	08 51 18	+11 50 06	0.58	0.07	0.27	0.04	13.0	0.1	12.4	0.1	12.1	0.1
140	08 51 02	+11 47 50	0.53	0.07	0.39	0.05	13.5	0.1	12.9	0.1	12.5	0.1
141	08 50 59	+11 48 58	0.58	0.08	0.37	0.06	13.5	0.2	13.0	0.1	12.6	0.2
142	08 51 17	+11 54 15	0.60	0.06	0.36	0.05	13.7	0.1	13.1	0.1	12.7	0.2
143	08 51 38	+11 50 57	0.49	0.08	0.40	0.06	13.5	0.1	13.0	0.1	12.6	0.1
144	08 50 55	+11 51 09	0.56	0.07	0.36	0.05	13.5	0.1	13.0	0.1	12.6	0.2
145	08 51 08	+11 50 08	0.57	0.09	0.39	0.07	13.6	0.2	13.0	0.1	12.6	0.2
146	08 50 53	+11 44 35	0.60	0.08	0.48	0.07	13.5	0.2	12.9	0.1	12.4	0.2
147	08 51 45	+11 56 55	0.52	0.07	0.30	0.06	13.6	0.2	13.1	0.1	12.8	0.2
148	08 51 36	+11 48 52	0.53	0.12	0.39	0.08	14.0	0.2	13.4	0.1	13.1	0.2
149	08 51 13	+11 50 35	0.45	0.45	0.07	0.39	13.1	0.8	12.6	0.5	12.6	0.8
150	08 51 14	+11 51 18	0.53	0.09	0.38	0.06	13.7	0.2	13.2	0.1	12.8	0.2
151	08 51 32	+11 55 09	0.59	0.09	0.36	0.05	13.9	0.2	13.3	0.1	12.9	0.1
152	08 50 53	+11 40 02	0.58	0.09	0.47	0.04	13.6	0.1	13.0	0.1	12.5	0.1
153	08 50 56	+11 53 52	0.54	0.07	0.36	0.06	13.7	0.2	13.2	0.1	12.8	0.2
154	08 50 53	+11 40 43	0.57	0.07	0.45	0.07	13.6	0.2	13.1	0.1	12.6	0.2
155	08 51 39	+11 47 55	0.61	0.08	0.44	0.06	13.8	0.2	13.2	0.1	12.7	0.2
156	08 51 19	+11 40 16	0.54	0.08	0.35	0.06	13.8	0.2	13.2	0.1	12.9	0.2
157	08 51 20	+11 50 23	0.53	0.20	0.51	0.11	14.2	0.3	13.7	0.1	13.2	0.2
158	08 51 34	+11 50 54	0.96	0.25	-0.61	0.19	14.3	0.4	13.3	0.2	13.9	0.4
159	08 51 19	+11 47 55	0.49	0.15	0.51	0.12	13.8	0.3	13.3	0.2	12.8	0.3
160	08 51 09	+11 50 53	0.55	0.10	0.35	0.07	14.0	0.2	13.4	0.1	13.1	0.2
161	08 51 31	+11 53 18	0.52	0.11	0.38	0.07	13.2	0.2	12.7	0.1	12.3	0.2
162	08 51 29	+11 48 02	0.36	0.32	0.86	0.31	13.6	0.6	13.3	0.4	12.4	0.7
163	08 50 59	+11 48 19	0.57	0.07	0.39	0.04	13.7	0.1	13.1	0.1	12.7	0.1
164	08 51 12	+11 48 51	0.58	0.09	0.40	0.06	13.9	0.2	13.3	0.1	12.9	0.2
165	08 51 41	+11 49 06	0.54	0.09	0.36	0.06	14.0	0.2	13.5	0.1	13.1	0.2
166	08 51 50	+11 45 00	0.56	0.07	0.35	0.06	13.0	0.2	12.4	0.1	12.1	0.2
167	08 51 05	+11 49 34	0.58	0.08	0.38	0.05	13.7	0.1	13.1	0.1	12.7	0.1
168	08 51 40	+11 52 43	0.51	0.07	0.38	0.06	13.8	0.2	13.3	0.1	12.9	0.2
169	08 51 26	+11 40 13	0.86	0.11	0.55	0.07	14.0	0.2	13.2	0.1	12.6	0.2
170	08 51 40	+11 46 38	0.53	0.09	0.38	0.06	13.9	0.2	13.4	0.1	13.0	0.2
171	08 51 20	+11 52 48	0.55	0.09	0.37	0.06	13.9	0.2	13.3	0.1	12.9	0.2
172	08 51 05	+11 52 26	0.55	0.07	0.35	0.06	13.8	0.2	13.2	0.1	12.9	0.2
173	08 51 20	+11 52 11	0.56	0.07	0.42	0.07	14.1	0.2	13.5	0.1	13.1	0.2
174	08 51 19	+11 49 24	0.47	0.16	0.38	0.12	12.6	0.3	12.2	0.2	11.8	0.3
175	08 51 56	+11 48 38	0.65	0.08	0.37	0.05	14.1	0.2	13.4	0.1	13.0	0.2
176	08 52 03	+11 58 05	0.47	0.08	0.27	0.12	14.1	0.3	13.7	0.2	13.4	0.4
177	08 51 55	+11 40 50	0.66	0.09	0.40	0.05	14.1	0.2	13.5	0.1	13.1	0.2
178	08 51 17	+11 46 03	0.52	0.09	0.52	0.08	13.2	0.2	12.6	0.2	12.1	0.2
179	08 51 09	+11 48 38	0.66	0.08	0.47	0.06	13.9	0.2	13.3	0.1	12.8	0.2
180	08 51 12	+11 48 35	0.65	0.10	0.33	0.05	13.9	0.2	13.2	0.1	12.9	0.1
181	08 51 37	+11 46 56	0.58	0.11	0.40	0.09	14.2	0.2	13.6	0.2	13.2	0.3
182	08 51 22	+11 51 42	0.59	0.09	0.41	0.10	14.1	0.2	13.5	0.2	13.1	0.3
183	08 51 06	+11 43 47	0.65	0.07	0.44	0.08	14.1	0.2	13.5	0.2	13.1	0.2
184	08 51 36	+11 56 51	0.53	0.07	0.25	0.11	14.2	0.3	13.7	0.2	13.4	0.3
185	08 51 04	+11 51 46	0.60	0.13	0.42	0.08	14.1	0.2	13.5	0.2	13.1	0.2
186	08 51 57	+11 48 12	0.55	0.08	0.31	0.05	14.1	0.2	13.5	0.1	13.2	0.1
187	08 51 39	+11 42 37	0.52	0.09	0.38	0.08	14.2	0.2	13.6	0.2	13.3	0.2
188	08 51 32	+11 51 17	0.54	0.09	0.40	0.11	14.3	0.3	13.7	0.2	13.3	0.3
189	08 51 41	+11 47 36	0.60	0.13	0.44	0.13	14.3	0.3	13.7	0.3	13.3	0.4
190	08 51 25	+11 45 43	0.56	0.18	0.49	0.10	14.5	0.3	13.9	0.2	13.5	0.3
191	08 51 19	+11 40 37	0.54	0.08	0.38	0.06	14.1	0.2	13.5	0.1	13.1	0.2
192	08 51 48	+11 42 23	0.52	0.08	0.36	0.08	14.1	0.2	13.6	0.2	13.2	0.2
193	08 51 30	+11 51 09	0.85	0.12	0.28	0.12	14.7	0.3	13.8	0.2	13.5	0.3
194	08 51 23	+11 48 27	0.64	0.20	0.50	0.14	13.3	0.3	12.7	0.2	12.2	0.3
195	08 51 19	+11 55 50	0.56	0.10	0.35	0.08	14.2	0.2	13.6	0.2	13.3	0.2
196	08 51 28	+11 53 02	0.78	0.17	0.39	0.09	14.7	0.3	14.0	0.2	13.6	0.3
197	08 51 25	+11 48 14	0.72	0.09	0.34	0.09	14.0	0.2	13.3	0.2	13.0	0.3
198	08 51 17	+11 45 42	0.71	0.28	0.95	0.22	12.8	0.5	12.1	0.3	11.1	0.5
199	08 51 12	+11 54 23	0.58	0.08	0.36	0.07	14.2	0.2	13.6	0.2	13.3	0.2
200	08 51 34	+11 46 56	0.52	0.11	0.39	0.09	14.5	0.2	14.0	0.2	13.6	0.3

Contd. Table A1: Results of photometry, Messier 67

No.	α	δ	m_{v-b}	σ_{v-b}	m_{b-y}	σ_{b-y}	m_v	σ_v	m_b	σ_b	m_y	σ_y
201	08 51 22	+11 44 05	0.70	0.10	0.54	0.08	14.2	0.2	13.5	0.1	13.0	0.2
202	08 50 56	+11 51 29	0.60	0.08	0.40	0.07	14.1	0.2	13.5	0.1	13.1	0.2
203	08 51 33	+11 48 24	0.58	0.15	0.20	0.19	14.5	0.4	13.9	0.3	13.7	0.5
204	08 51 09	+11 57 54	0.62	0.11	0.48	0.06	14.1	0.2	13.5	0.1	13.0	0.2
205	08 51 15	+11 49 21	-0.12	0.82	1.19	0.82	13.6	1.7	13.7	1.0	12.5	1.8
206	08 51 23	+11 54 05	0.60	0.09	0.38	0.07	14.3	0.2	13.7	0.2	13.3	0.2
207	08 50 53	+11 43 40	0.64	0.07	0.59	0.13	14.2	0.3	13.5	0.3	12.9	0.4
208	08 51 20	+11 51 02	0.61	0.15	0.38	0.10	14.7	0.3	14.0	0.2	13.7	0.3
209	08 51 59	+11 50 02	0.65	0.17	0.42	0.07	14.5	0.3	13.8	0.2	13.4	0.2
210	08 51 18	+11 50 20	0.69	0.08	0.41	0.07	14.1	0.2	13.4	0.1	13.0	0.2
211	08 51 47	+11 47 10	0.86	0.11	0.39	0.07	15.0	0.2	14.2	0.2	13.8	0.2
212	08 51 16	+11 48 16	0.92	0.13	0.20	0.15	14.4	0.3	13.5	0.2	13.3	0.4
213	08 52 00	+11 56 07	0.61	0.11	0.31	0.13	14.8	0.3	14.2	0.3	13.9	0.4
214	08 51 38	+11 56 45	0.61	0.09	0.24	0.07	14.7	0.2	14.1	0.2	13.9	0.2
215	08 51 25	+11 48 04	0.77	0.09	0.29	0.08	14.2	0.2	13.4	0.2	13.1	0.2
216	08 51 14	+11 49 59	0.40	0.22	0.51	0.21	14.6	0.5	14.2	0.4	13.7	0.6
217	08 51 27	+11 57 09	0.75	0.08	0.38	0.08	14.7	0.2	14.0	0.2	13.6	0.2
218	08 51 40	+11 42 55	0.56	0.07	0.39	0.06	14.4	0.2	13.8	0.1	13.4	0.2
219	08 51 24	+11 48 26	0.59	0.06	0.39	0.05	12.7	0.1	12.2	0.1	11.8	0.1
220	08 51 13	+11 57 01	0.59	0.12	0.29	0.12	14.8	0.3	14.2	0.3	13.9	0.4
221	08 51 28	+11 50 12	0.94	0.20	0.53	0.18	15.2	0.4	14.2	0.3	13.7	0.5
222	08 51 57	+11 47 25	0.61	0.17	0.29	0.13	14.8	0.3	14.2	0.3	13.9	0.4
223	08 51 36	+11 47 47	0.81	0.21	0.39	0.14	15.2	0.5	14.4	0.3	14.0	0.4
224	08 51 03	+11 51 25	0.90	0.12	0.50	0.05	14.9	0.2	14.0	0.1	13.5	0.2
225	08 51 04	+11 42 24	0.50	0.11	0.40	0.10	14.5	0.3	14.0	0.2	13.6	0.3
226	08 51 22	+11 43 18	0.57	0.12	0.44	0.11	14.6	0.2	14.1	0.2	13.6	0.3
227	08 51 33	+11 42 05	0.74	0.10	0.48	0.08	14.7	0.2	13.9	0.2	13.5	0.2
228	08 51 50	+11 39 58	1.67	0.76	0.70	0.13	15.9	0.6	14.2	0.2	13.5	0.3
229	08 51 14	+11 41 09	0.60	0.09	0.39	0.12	14.7	0.3	14.1	0.2	13.7	0.4
230	08 51 53	+11 56 17	0.82	0.14	0.35	0.13	15.0	0.3	14.2	0.3	13.9	0.4
231	08 51 49	+11 48 02	0.64	0.13	0.45	0.11	14.9	0.3	14.3	0.2	13.8	0.3
232	08 51 09	+11 57 00	0.60	0.13	0.26	0.09	14.9	0.2	14.3	0.2	14.1	0.2
233	08 51 17	+11 42 37	0.59	0.08	0.37	0.07	14.6	0.2	14.0	0.2	13.6	0.2
234	08 51 53	+11 54 19	0.88	0.23	0.24	0.13	15.6	0.4	14.7	0.3	14.5	0.4
235	08 51 32	+11 46 46	0.74	0.12	0.50	0.11	14.7	0.3	14.0	0.2	13.5	0.3
236	08 51 01	+11 48 53	0.75	0.19	0.40	0.08	14.9	0.3	14.2	0.2	13.8	0.3
237	08 50 57	+11 49 55	0.88	0.17	0.44	0.19	15.4	0.3	14.5	0.3	14.0	0.5
238	08 52 04	+11 47 48	0.68	0.13	0.53	0.11	14.5	0.3	13.9	0.2	13.3	0.3
239	08 51 10	+11 46 17	0.73	0.16	0.36	0.08	15.0	0.2	14.3	0.2	13.9	0.2
240	08 51 16	+11 40 30	0.79	0.21	0.54	0.08	14.8	0.3	14.0	0.2	13.5	0.2
241	08 51 25	+11 43 06	0.75	0.08	0.43	0.12	15.0	0.3	14.2	0.2	13.8	0.3
242	08 50 60	+11 44 08	0.91	0.14	0.47	0.04	15.1	0.2	14.2	0.2	13.7	0.2
243	08 51 35	+11 43 49	0.58	0.07	0.43	0.08	14.6	0.2	14.0	0.2	13.6	0.2
244	08 50 52	+11 45 04	0.68	0.16	0.60	0.10	14.4	0.3	13.8	0.2	13.2	0.3
245	08 51 26	+11 49 56	0.77	0.35	0.61	0.19	15.2	0.5	14.4	0.4	13.8	0.6
246	08 50 56	+11 51 56	0.93	0.12	-0.03	0.05	15.1	0.2	14.1	0.1	14.2	0.1
247	08 51 59	+11 41 49	0.79	0.20	0.34	0.06	15.3	0.2	14.5	0.1	14.1	0.2
248	08 51 47	+11 44 42	0.87	0.18	0.01	0.13	15.2	0.2	14.4	0.2	14.4	0.3
249	08 51 12	+11 48 27	0.59	0.09	0.35	0.11	13.9	0.2	13.3	0.2	12.9	0.3
250	08 51 32	+11 51 57	1.96	0.06	0.96	0.03	16.8	0.1	14.8	0.1	13.9	0.1
251	08 51 27	+11 47 33	0.03	0.67	0.37	0.34	15.7	0.8	15.6	0.5	15.3	0.7
252	08 51 01	+11 53 11	0.39	0.21	0.76	0.25	14.6	0.6	14.3	0.5	13.5	0.7
253	08 51 52	+11 44 50	1.17	0.38	0.23	0.07	16.1	0.5	14.9	0.2	14.7	0.2
254	08 51 41	+11 44 53	0.93	0.25	0.50	0.14	15.3	0.4	14.4	0.2	13.9	0.3
255	08 51 08	+11 51 57	0.59	0.17	0.76	0.10	14.8	0.2	14.2	0.2	13.4	0.3
256	08 51 09	+11 49 31	0.84	0.16	0.55	0.11	14.9	0.2	14.1	0.2	13.5	0.3
257	08 51 49	+11 47 36	0.69	0.16	0.42	0.19	15.3	0.5	14.6	0.3	14.2	0.5
258	08 51 12	+11 50 33	0.65	0.06	0.37	0.03	12.9	0.1	12.3	0.1	11.9	0.1
259	08 51 02	+11 49 27	0.59	0.07	0.43	0.05	12.5	0.1	11.9	0.1	11.5	0.2
260	08 50 57	+11 56 51	0.83	0.22	0.43	0.19	15.5	0.3	14.7	0.3	14.2	0.5
261	08 52 02	+11 55 34	0.78	0.13	0.58	0.07	14.8	0.2	14.1	0.2	13.5	0.2
262	08 50 60	+11 51 13	0.65	0.27	0.74	0.32	15.4	0.7	14.7	0.5	14.0	0.8
263	08 51 30	+11 51 22	0.54	0.14	0.37	0.06	13.3	0.2	12.7	0.1	12.3	0.2
264	08 51 34	+11 45 54	0.59	0.06	0.26	0.03	15.3	0.1	14.7	0.1	14.4	0.1
265	08 51 02	+11 56 16	0.64	0.07	0.48	0.13	14.9	0.3	14.3	0.2	13.8	0.4
266	08 51 42	+11 49 38	0.89	0.10	-0.12	0.08	15.3	0.2	14.4	0.1	14.5	0.2
267	08 51 24	+11 47 28	0.95	0.06	0.17	0.03	15.0	0.1	14.0	0.1	13.9	0.1
268	08 51 03	+11 52 26	0.77	0.23	0.27	0.08	15.8	0.4	15.0	0.2	14.8	0.2
269	08 51 24	+11 49 50	0.84	0.07	0.55	0.04	11.5	0.1	10.7	0.1	10.2	0.1
270	08 51 02	+11 45 19	0.44	0.06	0.46	0.03	14.8	0.1	14.3	0.1	13.8	0.1
271	08 51 12	+11 47 15	0.06	0.06	1.61	0.03	14.1	0.1	14.1	0.1	12.5	0.1
272	08 50 54	+11 55 15	0.94	0.06	0.47	0.03	15.6	0.1	14.7	0.1	14.2	0.1
273	08 51 15	+11 51 58	0.55	0.66	0.97	0.34	15.1	0.9	14.5	0.4	13.5	0.7
274	08 50 56	+11 52 56	0.89	0.09	0.38	0.07	15.5	0.1	14.6	0.2	14.2	0.3
275	08 51 43	+11 40 60	0.60	0.06	0.66	0.03	14.8	0.1	14.2	0.1	13.5	0.1
276	08 51 06	+11 53 11	0.71	0.19	0.30	0.16	15.4	0.4	14.7	0.3	14.4	0.4
277	08 51 33	+11 53 45	0.58	0.20	0.66	0.11	15.1	0.3	14.6	0.1	13.9	0.2
278	08 51 37	+11 54 27	0.88	0.07	0.53	0.05	15.7	0.1	14.8	0.1	14.3	0.1
279	08 51 56	+11 53 36	0.78	0.15	0.31	0.14	15.5	0.5	14.7	0.3	14.4	0.4
280	08 51 14	+11 44 37	0.87	0.06	-0.24	0.03	15.3	0.1	14.4	0.1	14.7	0.1

Contd. Table A1: Results of photometry, Messier 67

No.	α	δ	m_{v-b}	σ_{v-b}	m_{b-y}	σ_{b-y}	m_v	σ_v	m_b	σ_b	m_y	σ_y
281	08 52 01	+11 52 29	1.02	0.08	0.28	0.07	16.0	0.1	15.0	0.1	14.7	0.1
282	08 51 59	+11 51 14	0.50	0.07	0.56	0.13	15.2	0.3	14.7	0.2	14.2	0.4
283	08 51 59	+11 52 15	0.49	0.06	0.49	0.03	15.3	0.1	14.8	0.1	14.3	0.1
284	08 51 33	+11 45 60	0.60	0.12	0.62	0.28	15.0	0.6	14.4	0.5	13.8	0.8
285	08 51 27	+11 44 22	0.14	0.06	0.50	0.03	15.1	0.1	15.0	0.1	14.5	0.1
286	08 51 19	+11 50 14	0.58	0.07	0.36	0.04	12.6	0.1	12.0	0.1	11.7	0.1
287	08 51 37	+11 54 50	0.54	0.07	0.35	0.05	13.2	0.2	12.7	0.1	12.3	0.2
288	08 51 14	+11 57 34	0.89	0.06	0.33	0.03	16.0	0.1	15.1	0.1	14.8	0.1
289	08 51 37	+11 49 59	0.58	0.09	0.39	0.05	12.7	0.2	12.2	0.1	11.8	0.1
290	08 50 53	+11 49 46	1.28	0.06	0.75	0.03	15.7	0.1	14.4	0.1	13.7	0.1
291	08 50 55	+11 51 22	0.61	0.12	0.17	0.10	15.2	0.2	14.6	0.1	14.4	0.2
292	08 51 35	+11 51 39	0.58	0.06	0.37	0.03	16.1	0.1	15.5	0.1	15.2	0.1
293	08 51 53	+11 53 55	0.52	0.10	0.17	0.09	16.1	0.3	15.6	0.2	15.4	0.3
294	08 51 05	+11 49 36	0.58	0.08	0.38	0.05	13.7	0.1	13.1	0.1	12.7	0.1
295	08 51 02	+11 47 52	0.53	0.07	0.39	0.05	13.5	0.1	12.9	0.1	12.5	0.1
296	08 51 14	+11 44 41	0.87	0.06	-0.24	0.03	15.3	0.1	14.4	0.1	14.7	0.1
297	08 51 08	+11 56 31	0.64	0.06	0.12	0.03	16.2	0.1	15.6	0.1	15.4	0.1
298	08 51 29	+11 45 34	0.89	0.06	0.57	0.05	13.0	0.1	12.1	0.1	11.6	0.1
299	08 50 59	+11 48 29	0.57	0.07	0.40	0.05	13.7	0.1	13.1	0.1	12.7	0.1
300	08 51 02	+11 48 53	0.59	0.07	0.41	0.05	13.3	0.1	12.7	0.1	12.3	0.1
301	08 52 04	+11 58 09	0.47	0.08	0.27	0.12	14.1	0.3	13.7	0.2	13.4	0.4
302	08 51 22	+11 44 09	0.70	0.10	0.54	0.08	14.2	0.2	13.5	0.1	13.0	0.2
303	08 51 04	+11 51 40	0.59	0.13	0.42	0.08	14.1	0.2	13.5	0.2	13.1	0.2

5.7.2 Chupina 1

Table A2: Results of photometry, Chupina 1

No.	α	δ	m_{v-b}	σ_{v-b}	m_{b-y}	σ_{b-y}	m_v	σ_v	m_b	σ_b	m_y	σ_y
1	08 50 12	+11 51 24	1.65	0.06	0.91	0.04	9.37	0.1	7.7	0.1	6.8	0.1
2	08 50 02	+11 55 25	1.23	0.06	0.64	0.04	9.34	0.1	8.1	0.1	7.5	0.1
3	08 49 35	+11 51 26	1.43	0.06	0.80	0.04	9.93	0.1	8.5	0.1	7.7	0.1
4	08 50 18	+11 55 21	1.05	0.06	0.62	0.04	10.20	0.1	9.1	0.1	8.5	0.1
5	08 49 43	+11 48 39	0.47	0.06	0.30	0.04	10.56	0.1	10.1	0.1	9.8	0.1
6	08 49 37	+11 53 22	1.19	0.06	0.69	0.04	11.60	0.1	10.4	0.1	9.7	0.1
7	08 50 06	+11 57 51	1.08	0.06	0.60	0.04	11.74	0.1	10.7	0.1	10.1	0.1
8	08 49 57	+11 48 51	0.48	0.06	0.29	0.04	11.41	0.1	10.9	0.1	10.6	0.1
9	08 50 13	+11 57 29	0.48	0.06	0.26	0.04	11.70	0.1	11.2	0.1	11.0	0.1
10	08 49 46	+11 50 35	0.90	0.06	0.59	0.04	12.17	0.1	11.3	0.1	10.7	0.1
11	08 49 58	+11 55 53	0.52	0.06	0.30	0.04	12.51	0.1	12.0	0.1	11.7	0.1
12	08 49 27	+11 54 42	1.05	0.06	0.60	0.05	13.17	0.1	12.1	0.1	11.5	0.1
13	08 50 16	+11 53 48	0.51	0.07	0.32	0.05	12.91	0.1	12.4	0.1	12.1	0.1
14	08 50 34	+11 46 27	0.50	0.06	0.22	0.04	13.14	0.1	12.6	0.1	12.4	0.1
15	08 49 22	+12 01 52	0.95	0.06	-0.03	0.03	13.51	0.1	12.6	0.1	12.6	0.1
16	08 49 22	+12 01 54	0.95	0.06	-0.03	0.03	13.51	0.1	12.6	0.1	12.6	0.1
17	08 49 56	+11 53 41	0.75	0.06	0.44	0.06	13.44	0.1	12.7	0.1	12.2	0.2
18	08 49 57	+11 56 53	0.54	0.06	0.36	0.04	13.27	0.1	12.7	0.1	12.4	0.1
19	08 50 27	+11 48 31	0.57	0.06	0.29	0.06	13.53	0.1	13.0	0.1	12.7	0.2
20	08 49 48	+11 58 51	0.57	0.06	0.33	0.04	13.40	0.1	12.8	0.1	12.5	0.1
21	08 50 02	+12 00 32	0.52	0.06	0.31	0.03	13.38	0.1	12.9	0.1	12.5	0.1
22	08 50 00	+11 56 48	0.51	0.06	0.35	0.04	13.54	0.1	13.0	0.1	12.7	0.1
23	08 49 46	+11 56 36	0.63	0.06	0.36	0.03	13.71	0.1	13.1	0.1	12.7	0.1
24	08 49 45	+12 02 27	0.52	0.06	0.31	0.05	13.59	0.1	13.1	0.1	12.8	0.1
25	08 50 24	+11 48 57	0.42	0.06	0.27	0.06	13.57	0.1	13.2	0.1	12.9	0.2
26	08 50 20	+11 49 11	0.49	0.06	0.32	0.04	13.64	0.1	13.2	0.1	12.8	0.1
27	08 49 32	+11 57 20	0.68	0.06	0.40	0.03	13.93	0.1	13.2	0.1	12.8	0.1
28	08 50 10	+11 59 54	0.62	0.07	0.33	0.04	14.05	0.1	13.4	0.1	13.1	0.1
29	08 50 28	+11 54 51	0.57	0.06	0.46	0.05	14.07	0.1	13.5	0.1	13.0	0.1
30	08 50 19	+12 02 37	0.60	0.07	0.25	0.04	14.66	0.1	14.1	0.1	13.8	0.1
31	08 49 35	+11 47 17	0.76	0.09	0.34	0.05	14.61	0.1	13.8	0.1	13.5	0.1
32	08 50 26	+11 57 20	0.54	0.07	0.30	0.10	14.43	0.2	13.9	0.2	13.6	0.3
33	08 50 26	+12 02 10	0.93	0.08	0.31	0.03	15.16	0.1	14.2	0.1	13.9	0.1
34	08 49 53	+12 02 05	0.55	0.08	0.37	0.16	14.43	0.3	13.9	0.3	13.5	0.4
35	08 50 22	+11 50 23	0.62	0.08	0.39	0.05	14.67	0.1	14.0	0.1	13.7	0.1
36	08 50 33	+11 49 02	0.58	0.07	0.30	0.03	14.75	0.1	14.2	0.1	13.9	0.1
37	08 49 48	+11 57 50	0.85	0.17	0.37	0.19	15.04	0.5	14.2	0.3	13.8	0.5
38	08 49 58	+11 56 17	0.52	0.06	0.36	0.04	14.39	0.1	13.9	0.1	13.5	0.1
39	08 50 23	+11 51 59	0.65	0.06	0.48	0.03	14.70	0.1	14.1	0.1	13.6	0.1
40	08 49 43	+11 55 29	0.58	0.07	0.39	0.07	14.74	0.2	14.2	0.1	13.8	0.2
41	08 49 56	+11 52 52	0.86	0.06	0.52	0.03	14.84	0.1	14.0	0.1	13.5	0.1
42	08 50 18	+11 54 24	0.62	0.09	0.41	0.09	14.78	0.3	14.2	0.2	13.8	0.3
43	08 49 46	+11 58 45	0.60	0.08	0.52	0.17	14.69	0.3	14.1	0.4	13.6	0.5
44	08 49 33	+11 59 05	0.68	0.06	0.41	0.03	15.11	0.1	14.4	0.1	14.0	0.1
45	08 49 42	+11 55 15	0.69	0.15	0.38	0.05	14.81	0.1	14.1	0.1	13.7	0.2
46	08 49 49	+11 50 50	0.48	0.15	0.30	0.11	14.81	0.3	14.3	0.2	14.0	0.3
47	08 49 55	+11 58 12	0.79	0.06	0.43	0.03	15.36	0.1	14.6	0.1	14.1	0.1
48	08 50 20	+11 45 45	0.54	0.06	0.44	0.03	15.00	0.1	14.5	0.1	14.0	0.1
49	08 50 06	+11 49 32	0.45	0.16	0.44	0.09	14.82	0.3	14.4	0.2	13.9	0.3
50	08 50 17	+11 54 47	0.60	0.07	0.44	0.04	15.01	0.1	14.4	0.1	14.0	0.1
51	08 50 01	+11 56 28	0.68	0.06	0.69	0.03	15.18	0.1	14.5	0.1	13.8	0.1
52	08 50 21	+11 58 37	0.41	0.06	0.70	0.03	14.89	0.1	14.5	0.1	13.8	0.1
53	08 50 07	+11 48 12	0.03	0.06	0.58	0.03	14.73	0.1	14.7	0.1	14.1	0.1
54	08 50 00	+11 58 14	0.24	0.10	0.35	0.10	15.92	0.2	15.7	0.3	15.3	0.3
55	08 49 58	+11 56 11	0.48	0.12	0.37	0.09	14.35	0.3	13.9	0.2	13.5	0.2

5.7.3 Chupina 2

Table A3: Results of photometry, Chupina 2

No.	α	δ	m_{v-b}	σ_{v-b}	m_{b-y}	σ_{b-y}	m_v	σ_v	m_b	σ_b	m_y	σ_y
1	08 50 44	+12 07 41	1.60	0.06	1.04	0.03	9.95	0.1	8.3	0.1	7.3	0.1
2	08 50 21	+12 21 12	1.26	0.06	0.72	0.03	10.82	0.1	9.6	0.1	8.8	0.1
3	08 50 50	+12 17 16	0.77	0.06	0.53	0.03	11.66	0.1	10.9	0.1	10.4	0.1
4	08 50 34	+12 19 40	0.57	0.06	0.41	0.03	11.57	0.1	11.0	0.1	10.6	0.1
5	08 50 43	+12 11 37	1.01	0.06	0.67	0.03	12.43	0.1	11.4	0.1	10.8	0.1
6	08 50 50	+12 24 02	0.48	0.06	0.31	0.03	12.27	0.1	11.8	0.1	11.5	0.1
7	08 50 41	+12 17 00	0.64	0.06	0.53	0.03	12.36	0.1	11.7	0.1	11.2	0.1
8	08 50 29	+12 19 04	0.53	0.06	0.41	0.03	12.47	0.1	11.9	0.1	11.5	0.1
9	08 50 58	+12 18 32	0.55	0.06	0.39	0.03	12.58	0.1	12.0	0.1	11.6	0.1
10	08 50 30	+12 08 07	0.52	0.06	0.44	0.04	12.47	0.1	12.0	0.1	11.5	0.1
11	08 50 12	+12 09 38	0.64	0.06	0.50	0.03	12.56	0.1	11.9	0.1	11.4	0.1
12	08 50 47	+12 10 13	0.59	0.06	0.44	0.03	12.63	0.1	12.0	0.1	11.6	0.1
13	08 50 24	+12 19 59	0.51	0.06	0.36	0.03	12.64	0.1	12.1	0.1	11.8	0.1
14	08 50 56	+12 14 11	0.57	0.06	0.41	0.03	12.87	0.1	12.3	0.1	11.9	0.1
15	08 50 39	+12 07 46	0.54	0.07	0.39	0.05	13.17	0.1	12.6	0.1	12.2	0.1
16	08 50 33	+12 10 16	0.56	0.06	0.41	0.03	13.17	0.1	12.6	0.1	12.2	0.1
17	08 51 04	+12 08 25	0.50	0.06	0.36	0.03	13.32	0.1	12.8	0.1	12.5	0.1
18	08 50 56	+12 09 29	0.48	0.06	0.31	0.03	13.35	0.1	12.9	0.1	12.6	0.1
19	08 50 18	+12 17 17	0.53	0.06	0.42	0.03	13.11	0.1	12.6	0.1	12.2	0.1
20	08 50 38	+12 07 20	0.51	0.07	0.37	0.04	13.70	0.1	13.2	0.1	12.8	0.1
21	08 50 54	+12 15 34	0.53	0.06	0.38	0.03	13.58	0.1	13.1	0.1	12.7	0.1
22	08 50 44	+12 23 30	0.60	0.06	0.40	0.04	13.74	0.1	13.1	0.1	12.8	0.1
23	08 50 10	+12 17 43	0.64	0.06	0.47	0.03	13.83	0.1	13.2	0.1	12.7	0.1
24	08 50 35	+12 08 31	0.51	0.07	0.43	0.03	13.86	0.1	13.4	0.1	12.9	0.1
25	08 50 15	+12 20 27	0.91	0.08	0.60	0.04	14.20	0.1	13.3	0.1	12.7	0.1
26	08 50 40	+12 14 38	0.65	0.06	0.52	0.05	13.89	0.1	13.2	0.1	12.7	0.1
27	08 50 38	+12 19 50	0.70	0.07	0.45	0.04	14.22	0.1	13.5	0.1	13.1	0.1
28	08 50 57	+12 09 08	1.15	0.06	0.57	0.04	14.68	0.1	13.5	0.1	13.0	0.1
29	08 50 31	+12 06 56	0.62	0.07	0.55	0.10	14.19	0.2	13.6	0.2	13.0	0.2
30	08 50 32	+12 15 17	0.52	0.06	0.43	0.07	13.93	0.2	13.4	0.1	13.0	0.2
31	08 50 23	+12 13 37	0.57	0.07	0.48	0.08	14.03	0.2	13.5	0.2	13.0	0.2
32	08 50 19	+12 16 01	0.61	0.07	0.44	0.05	14.09	0.1	13.5	0.1	13.0	0.1
33	08 50 12	+12 14 34	0.58	0.06	0.46	0.04	14.04	0.1	13.5	0.1	13.0	0.1
34	08 51 02	+12 08 02	0.50	0.07	0.30	0.07	14.17	0.2	13.7	0.1	13.4	0.2
35	08 50 16	+12 19 34	0.70	0.08	0.45	0.04	13.75	0.1	13.0	0.1	12.6	0.1
36	08 50 16	+12 19 44	0.64	0.06	0.58	0.03	13.65	0.1	13.0	0.1	12.4	0.1
37	08 50 46	+12 10 40	0.79	0.10	0.53	0.03	14.79	0.2	14.0	0.1	13.5	0.1
38	08 50 54	+12 14 28	0.45	0.09	0.38	0.05	14.59	0.2	14.1	0.1	13.8	0.1
39	08 50 60	+12 18 55	0.51	0.06	0.41	0.07	14.49	0.2	14.0	0.2	13.6	0.2
40	08 50 35	+12 11 59	0.43	0.06	0.59	0.03	14.82	0.1	14.4	0.1	13.8	0.1
41	08 50 36	+12 08 52	0.47	0.06	0.65	0.03	14.53	0.1	14.1	0.1	13.4	0.1
42	08 50 46	+12 07 02	0.43	0.06	0.27	0.13	15.53	0.2	15.1	0.2	14.8	0.4
43	08 50 06	+12 09 10	0.44	0.06	0.46	0.12	14.74	0.3	14.3	0.2	13.8	0.3
44	08 50 03	+12 10 50	0.47	0.19	0.39	0.13	14.87	0.4	14.4	0.3	14.0	0.4
45	08 50 34	+12 22 37	0.58	0.06	0.35	0.03	15.25	0.1	14.7	0.1	14.3	0.1
46	08 50 04	+12 22 58	0.62	0.06	0.52	0.03	15.02	0.1	14.4	0.1	13.9	0.1
47	08 50 52	+12 17 32	0.35	0.06	0.44	0.03	14.86	0.1	14.5	0.1	14.1	0.1
48	08 50 45	+12 11 17	0.33	0.06	0.44	0.03	15.09	0.1	14.8	0.1	14.3	0.1
49	08 50 11	+12 11 04	1.22	0.06	0.47	0.03	15.89	0.1	14.7	0.1	14.2	0.1
50	08 50 55	+12 09 34	0.53	0.06	0.03	0.03	15.46	0.1	14.9	0.1	14.9	0.1
51	08 49 57	+12 17 20	0.91	0.06	0.62	0.03	15.50	0.1	14.6	0.1	14.0	0.1
52	08 50 08	+12 19 19	1.11	0.06	0.52	0.03	15.56	0.1	14.4	0.1	13.9	0.1
53	08 50 47	+12 12 38	0.51	0.10	0.32	0.10	15.47	0.2	15.0	0.1	14.6	0.2
54	08 51 07	+12 13 19	0.86	0.06	0.18	0.03	16.47	0.1	15.6	0.1	15.4	0.1
55	08 50 14	+12 15 05	0.76	0.06	0.96	0.03	15.11	0.1	14.4	0.1	13.4	0.1
56	08 50 18	+12 17 12	0.54	0.06	0.42	0.03	13.12	0.1	12.6	0.1	12.2	0.1

Bibliography

[1] Mark Allison, *Star Clusters and How to Observe Them*, Springer-Verlag London Limited (2006), 9-10.

[2] John K. Taylor, *Eclipsing binary stars in open clusters*, School of Chemistry and Physics, University of Keele (March 2006), 77.

[3] Hana Marková, *CCD fotometrie vybrané otevřené hvězdokupy II*, Přírodovědecká fakulta Masarykovy univerzity (2008), 7.

[4] Mark Allison, *Star Clusters and How to Observe Them*, Springer-Verlag London Limited (2006), 16.

[5] Dias W. S., Alessi B. S., Moitinho A. and Lépine J. R. D., 2002, A & A 389, 871.

[6] John K. Taylor, *Eclipsing binary stars in open clusters*, School of Chemistry and Physics, University of Keele (March 2006), 78.

[7] Doc. Dr. Bohumil Hacar, *Úvod do obecné astronomie*, Státní pedagogické nakladatelství, n.p., Praha (1963), 326.

[8] Doc. Dr. Bohumil Hacar, *Úvod do obecné astronomie*, Státní pedagogické nakladatelství, n.p., Praha (1963), 332.

[9] Mikulášek, Z., Krtička, J.: *Úvod do fyziky hvězd*, skripta, ÚTFA PřF MU, Brno (2005), 30.

[10] Mikulášek, Z., Krtička, J.: *Úvod do fyziky hvězd*, skripta, ÚTFA PřF MU, Brno (2005), 28.

[11] Johnson, H. L.; Morgan, W. W., *Fundamental stellar photometry for standards of spectral type on the revised system of the Yerkes spectral atlas*, The Astrophysical Journal, vol. 117, 1953, 313-352.

[12] Strömgren, Bengt, *Two-dimensional spectral classification of F stars through photoelectric photometry with interference filters*, Vistas in Astronomy, Vol. 2, Issue 1, 1956, 1336-1346

[13] Crawford, David L., *Two-Dimensional Spectral Classification by Narrow-Band Photometry for B Stats in Clusters and Associations*, Astrophysical Journal, Vol. 128, September 1958, 185-206

[14] Hermanec, Petr, *Základy astronomie a astrofyziky II*, skripta, Astronomický ústav Univerzity Karlovy, Praha (2012), 35

[15] Mikulášek, Z., Krtička, J.: *Úvod do fyziky hvězd*, skripta, ÚTFA PřF MU, Brno (2005), 33.

[16] Rosenberg, Hans (1910): *Über den Zusammenhang von Helligkeit und Spektraltypus in den Plejaden*, Astronomische Nachrichten 186 (4445), 71-78.

[17] Russell, Henry Norris (1914): *Relations Between the Spectra and Other Characteristics of the Stars*, Popular Astronomy 22, 275-294.

[18] Morgan, William Wilson; Keenan, Philip Childs; Kellman, Edith: *An atlas of stellar spectra, with an outline of spectral classification*, Chicago, Ill. (1943), The University of Chicago press

[19] A.S.Eddington, *The Internal Constitution of the Stars*, Cambridge University Press (1926)

[20] Balaguer-Núñez L., Galadí-Enriquez D., Jordi C., *uvby- Hβ CCD photometry and membership segregation of the open cluster NGC 2682 (M 67)*, Astron. Astrophys. (2007), 470, 585.

[21] Clem et al., *Empirically constrained color-temperature relations. II. uvby*, The Astronomical Journal (2004), 127:1227-1256.

[22] Harvey B. Richer, Gregory G. Fahlman, Joanne Rosvick, Rodrigo Ibata, *The White Dwarf Cooling Age of M67*, The Astronomical Journal (1998), 504.

[23] Krone-Martins A., Sourbiran C., Ducourant C., Teixeira R., Le Campion J. F., *Kinematic parameters and membership probabilities of open clusters in the Bordeaux PM2000 catalogue.*, Astron. Astriphys. (2010), 516, A3.

[e1] http://www.astro.cz/apod/ap130501.html

[e2] http://sfaaa-cms.hein-site.net/gallery3/Members_Gallery/Bob-Everson/My-first-year-of-Astrophotography/M45-080709-Pleiades-Open-Cluster-Area-51-Super-Takumar-135mm-SXVF-H9C

[e3] http://spiff.rit.edu/classes/phys445/lectures/colors/bessel_bandpass.gif

[e4] http://ulisse.pd.astro.it/Astro/ADPS/Systems/

[e5] http://obswww.unige.ch/gcpd/ph04.html

[e6] http://obswww.unige.ch/gcpd/filters/fil04.html

[e7] http://imagine.gsfc.nasa.gov/docs/teachers/lifecycles/Image31.gif

[e8] https://www.e-education.psu.edu/astro801/files/astro801/image/Lesson%207/zams.gif

[e9] http://www.nobelprize.org/nobel_prizes/physics/laureates/2009/index.html

[e10] http://www.univie.ac.at/webda/cgi-bin/ocl_page.cgi?dirname=chu01

[e11] http://www.univie.ac.at/webda/cgi-bin/ocl_page.cgi?dirname=chu02

[e12] http://www.univie.ac.at/webda/cgi-bin/ocl_page.cgi?dirname=ngc2682

[e13] http://munipack.physics.muni.cz

[e14] http://univie.ac.at/webda/cgi-bin/ocl_page.cgi?cluster=M67

[e15] http://archive.stsci.edu/cgi-bin/dss_form